

# Adhesion of Cells

P. BONGRAND

*Laboratoire d'Immunologie,  
Hôpital de Sainte-Marguerite,  
BP29, 13277 Marseille Cedex 09, France*

# Contents

1. Introduction .....	757
2. Representative models of cell adhesion .....	758
2.1. Interaction between cytotoxic T lymphocytes and target cells .....	758
2.2. Neutrophil adhesion to endothelium .....	761
2.3. Interactions between cells and artificial surfaces .....	764
3. Biophysical characterization of cells .....	769
3.1. Cell shape control .....	770
3.2. Cell surface roughness: the submicrometer scale .....	773
3.3. Relevance of the concept of surface tension to biological membranes .....	776
3.4. Molecular structure of the cell surface .....	777
4. Models for the sequential steps of cell adhesion .....	783
4.1. Cell-cell approach .....	783
4.2. Initiation of adhesion .....	790
4.3. Analysis of the 'equilibrium' shape of cell-cell contacts .....	794
4.4. Cell-cell separation .....	795
Conclusion .....	796
References .....	796

## 1. Introduction

Cell adhesion is a fascinating process. First, it plays a key role in many situations of biological and medical interest. Secondly, it is probably the best cell function to be considered for biophysical modeling from the micrometer to the molecular level. Thirdly, studying the biophysical aspects of cell adhesion leads to face many important problems of physics and physical chemistry as well as cell physiology.

There are at least two ways of approaching the problem of cell adhesion. A first strategy would be to perform a thorough study of a simplified model likely to share some fundamental properties with biological systems. Far reaching results were obtained along this line by studying adherence-induced deformations of individual conjugates made between lipid vesicles and/or red cells of known mechanical properties [28, 66]. As another example, detailed studies of the motion of antibody-coated red blood cells in controlled hydrodynamic flow yielded important information on the formation and rupture of intercellular bonds [169].

The aforementioned approaches yielded very useful data, and improved both biological and physical knowledge. However, several parameters likely to influence the adhesive properties of nucleated cells cannot be explored with model vesicles or even erythrocytes. Thus, the lateral displacements of adhesion molecules depend on cytoskeletal constraints [168] and active cell processes [176] that are clearly quite different in blood leukocytes and red cells. Further, whereas erythrocytes are fairly smooth at the submicrometer level, nucleated cells are studded with a variety of protrusions, blebs, ruffles, microvilli or lamellipodia with complex mechanical behavior and an obvious influence on adhesive interactions [129]. It seems therefore warranted to study biologically relevant models with available experimental and theoretical tools, even if data interpretation is less clearcut than with simpler systems. Indeed, understanding cell adhesion first requires that we identify the key parameters influencing this process and obtain reliable order-of-magnitude estimates for them.

The aim of the present review is to gather biological and biophysical data that are widely scattered in the literature, in order to allow biophysicists with a general knowledge of cell biology to assess the relevance of current physical concepts to cell adhesion. Hopefully, this might be useful to anyone willing to start research in this field. Therefore, we refer the reader to other reviews for a basic description of intermolecular forces [98] and their relevance to biological systems [22–24] as well as methods for studying cell adhesion [42].

First, we shall discuss some biological models of cell adhesion (with a bias related to the author's field of interest) in order to convey a quantitative feeling for the phenomena we are willing to study.

Secondly, we shall review some experimental data that may help build a working model of the basic 'adhering cell'.

Thirdly, we shall discuss the sequential steps of cell adhesion and current physical theories that are relevant to the involved mechanisms.

## 2. Representative models of cell adhesion

It is difficult to describe cell adhesion in some detail without referring to well defined biological models. Indeed, quite different parameters are expected to play a critical role in diverse situations. For example, the rapid adhesion of leukocytes to endothelial cells in flowing blood should not be modeled in the same way as the slow spreading of fibroblasts on culture dishes.

We shall describe three models of potential interest for biophysicists with some basic references allowing easier access to recent literature. Completeness was deliberately sacrificed for the sake of clarity.

### 2.1. Interaction between cytotoxic T lymphocytes and target cells

Cytotoxic T lymphocytes (CTLs) are able to recognize specific targets with exquisite specificity. Thus, they can detect infected cells expressing minute amounts of viral components on their membrane. The cytotoxic process involves sequential steps that were described in several excellent reviews [18, 93]. First, the CTL binds to the target, forming a 'conjugate' (fig. 1). Then, during the following 10–15 minutes, it inflicts on the target an irreversible damage, called the 'lethal hit': this probably includes a combination of events such as secretion of lytic molecules (e.g., perforin), fas-based signalling, possibly mechanical damage [86, 93]. The lethal hit does not provoke immediate morphological transformation of the target [93, 181]. However, a few tens of minutes after the recognition stage, the CTL spontaneously separates from its prey [148] which will disintegrate during the following 2–3 hours.

Many studies were devoted to the binding stage of T cell-mediated cytotoxicity. Adhesion may occur within a few seconds after intercellular contact, and electron microscopy revealed tight interactions between membranes in contact areas [103]. In a quantitative kinetic study, CTLs and target cells were centrifuged and different samples were processed at regular intervals for optical and electron microscopical study [76]. Numerous conjugates were found as soon as 60 seconds after contact formation, with a maximum 30 minutes later. Maximum membrane apposition was achieved within one minute, with apparent contact areas of the order of 10–20  $\mu\text{m}^2$ . (These areas were defined as the regions where CTL and target membranes were separated by a gap thinner than 250 nm on electron micrographs.)

In other series of experiments, the mechanical strength of adhesion was estimated by subjecting conjugates to calibrated laminar flows of increasing velocity. The shear rate required to disrupt 50% of conjugates was about 100,000  $\text{s}^{-1}$  [26, 27], corresponding to a maximum separating force of [22]:

$$F = 19.2\mu a^2 G = 3 \times 10^{-8} \text{ newton} \quad (1)$$

where  $\mu$  is the medium viscosity,  $a$  is the cell radius and  $G$  is the shear rate. This represents an upper limit for the actual separating force since cell doublets were

Fig. 1. Interaction between a cytotoxic *T* lymphocyte and target cell. A typical conjugate made between a murine cytotoxic *T* lymphocyte (CTL) of C57BL/6 origin and a specific target cell (S194 myeloma cell) was processed for electron microscopy as described in ref. [76]. Extensive membrane apposition is apparent in the contact area. Bar is 1  $\mu\text{m}$ .

probably oriented at random with respect to the velocity gradient, and this gradient was not spatially uniform. It was shown that this force was close to the cell membrane resistance, and conjugate disruption was often associated to target rupture [26].

In other studies [165, 172], conjugates were formed between individual CTLs and targets maintained on the tip of glass micropipettes by moderate aspiration. After 10 minute contact, the pipette holding the CTL was pulled away by micromanipulation, with increasing pressure. The minimal aspiration pressure required to break the conjugate was recorded. The maximal axial pipette force was about  $4 \times 10^{-9}$  N. This is not inconsistent with hydrodynamic data since

- i) marked differences are found between diverse populations of CTLs and target cells, and
- ii) the hydrodynamic force was exerted on the conjugates during a very brief time, and an inverse relationship was found between the minimum intensity and duration of application of the force required to rupture cell-substrate bonds [128].

In addition to the availability of quantitative data, the CTL model is of particular interest since extensive studies were devoted to the identification of adhesion molecules involved in conjugate formation. Adhesion is indeed achieved by combination of several binding mechanisms. See table 1 for more information on some important adhesion molecules.

Table 1  
Properties of some molecules involved in leukocyte adhesion.

Name	Distribution	Ligand(s)	Length (nanometer)	Structure	Functional properties	Reference
Intercellular adhesion molecule 1 (ICAM-1)	Leukocyte, endothelium	LFA-1	18.7	single chain 90–110 kd		[160, 161]
Lymphocyte, function associated 1 (LFA-1, CD11a/CD18)	Leukocytes	ICAM-1, 2, 3	20	$\alpha$ chain 180 kd $\beta$ 2 chain 95 kd	regulated by cell activation transduces costimulatory signal	[97, 160]
E-selectin (ELAM-1)	Endothelial cells	sialyl lewis X	28	protein 115 kd		[19, 160]
T cell receptor	T lymphocytes	peptide+ histocompatibility molecule	8	multichain, recognition by heterodimer 2 $\times$ 30 kd	several activation pathways	[182]
CD8 (Lyt2/Lyt3)	T lymphocyte subpopulation	class I histocompatibility	$\approx$ 20	homomultimer 34 kd	adhesion+signal transduction	[20, 160]
Major histocompatibility class I molecules (HLA-A, B, C)	ubiquitous	peptide and CD8	< 10	$\beta$ 2-microglobulin + $\alpha$ chain 45 kd	Signal ?	[21]

We list some properties of adhesion molecules referred to in text. ICAM-1 belongs to the immunoglobulin superfamily. LFA-1 is a  $\beta$ 2 integrin found on leukocytes together with MAC-1 (Mo1, CR3, CD11b/CD18) and p150/95 (CD11c/CD18). The recently defined selectin family includes E-selectin, P-selectin (CD62, PADGEM, GMP140), transiently expressed by activated platelets and endothelial cells, and L-selectin (LAM-1, MEL-14) expressed on leukocytes.

L-selectin is the major ligand of E-selectin on neutrophils.

First, specific recognition results from the association between T-cell receptors on the CTL and antigenic structures on the target. In physiological situations, these structures are usually complexes made between class I major histocompatibility complex (MHC) molecules and oligopeptides resulting from partial degradation of foreign material. In this case, only a minor fraction of the hundreds of thousands of MHC molecules [112] on the target membrane may be associated to a polypeptide antigen. Indeed, as few as 200 such complexes may suffice to allow recognition [35]. However, for practical reasons, many experiments were done with CTLs specific for allogeneic cells. In this case, a different proportion of target MHC class I molecules may serve as binding sites (this was the case in aforementioned determinations of binding strength).

The exquisite sensitivity of CTL recognition is due to the frequent involvement of accessory ligand molecules. Thus, CD8 molecules on the CTL will bind MHC class I molecules on the target. It was indeed shown that the overexpression of CD8 on transfected cell lines was sufficient to induce conjugate formation [139]. The accessory role of CD8/MHC interaction in CTL-target binding is supported by experimental data suggesting that CTLs with high affinity antigen receptor were less dependent on CD8 than CTLs with lower affinity [110].

In addition, CTLs are endowed with several accessory antigen-independent adhesion pathways [158]. LFA-1 molecules expressed on the CTL membrane will bind to ICAM molecules that are present on many target cells (table 1). A peculiarity of this adhesion system is that LFA-1 molecules must be activated before they can bind their ligand. Many activation pathways were described, including T-cell receptor (TCR) engagement after ligand recognition [140]. Other adhesive couples, such as CD2 (on the CTL) versus LFA3 (on the target) were described [158]. However, a more complete description of CTL adhesion would not fall within the scope of the present review.

A final point of interest in this model is the demonstration that conjugate formation usually results in marked redistribution of adhesion-involved and adhesion-independent molecules in cell-cell contact area. This redistribution was expected as a thermodynamic consequence of binding affinity and lateral mobility of membrane molecules [16]. Further, micromanipulation experiments showed that the affinity between CTL and target membranes increased when the contact area decreased, during contact disruption [172], which might be viewed as a consequence of the increase of bond density in the shrinking contact area. Finally, qualitative [109] and quantitative [6] immunofluorescence studies demonstrated about twofold increase of adhesion molecules in contact areas between target cells and CTLs.

## 2.2. Neutrophil adhesion to endothelium

The adhesion of blood granulocytes (fig. 2) is of high interest for several reasons. First, this is a key event in acute inflammation. Secondly, our knowledge of the adhesion molecules involved in this model exhibited a dramatic progress during the last few years [191]. Thirdly, many biophysical studies were done on the mechanical properties of blood granulocytes [134], thus allowing easier elaboration of quantitative models for adhesion. Fourthly, the physiological conditions of granulocyte

adhesion are relatively well known. Indeed, many remarkable studies were done on blood flow in capillary vessels, using intravital microscopy [11, 123, 154, 166]. This point is of importance, since it is now widely accepted that different binding molecules can be involved in adhesion at rest and under dynamic conditions [14]. Here are some points of interest.

In normal blood, about 50% of granulocytes are adhering to the vessel surface (this is the so-called margined pool), and half are flowing. Local adhesion may be rapidly induced by a complex modulation of the expression of adhesive molecules on the surfaces of granulocytes and endothelial cells.

There are two main groups of adhesive interactions [191]: first, leukocyte  $\beta 2$ -integrins (i.e. LFA1 also called CD11a/CD18, Mac-1 or CD11b/CD18, and p150-95 or CD11c/CD18) will bind ICAMs that are constitutively expressed on endothelial cells (table 1). As mentioned above, some kind of leukocyte activation is required for this binding. Secondly, lectin-sugar interactions may occur. Lectin molecules are inducible P-selectin (GMP140, CD62, PADGEM) and E-selectin (ELAM-1) on endothelial cells and L-selectin (LAM-1) constitutively expressed by neutrophils (see [160] for an illuminating review on these adhesion molecules). All these selectins were recently reported to recognize a common carbohydrate epitope that may be expressed by different molecules on cell membranes [77].

Now, leukocyte-endothelium adhesion is expected to be easiest in postcapillary venules where the shear rate  $G$  is minimal (see fig. 3 for definitions). Reported values of the wall shear rate  $G_w$  in these venules range between 100 and 1000  $s^{-1}$  [11, 123, 154, 166]. According to the definition of  $G_w$ , the fluid velocity at distance  $d$  from the vessel wall is the product  $G_w d$ . As will be explained below, the velocity of a cell of radius  $a$  close to the vessel surface is expected to be in the order of

Fig. 2. Granulocyte-endothelium interaction in a laminar chamber flow. Human granulocytes (arrow) were subjected to a laminar shear flow (shear rate  $4 s^{-1}$ ) in a previously described chamber [170]. The chamber floor is coated with human umbilical endothelial cells [193]. Bar is 10  $\mu m$ .

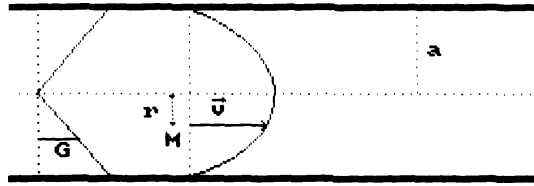


Fig. 3. Laminar flow through a cylindrical pipe. The velocity  $\vec{v}$  is everywhere parallel to the duct axis. At any point  $M$  separated from this axis by a distance  $r$ , one has  $v(r) = 2Q(a^2 - r^2)/\pi a^4$ , where  $Q$  is the flow rate (in  $\text{m}^3/\text{s}$ ) and  $a$  the duct radius. The velocity is thus zero at the wall and attains its maximum on the axis. The shear rate  $G = |dv/dr|$  is linearly dependent on  $r$ , with its maximum value at the wall and zero value on the axis.

$G_w a$  if there is no tight apposition between the cell and the endothelium. Hence, the velocity of a typical flowing granulocyte of radius  $4 \mu\text{m}$  is expected to be higher than several hundreds of  $\mu\text{m}/\text{s}$ . Also, the viscous force exerted on a bound spherical cell of radius  $a$  is [22]

$$F = 32\mu a^2 G_w \quad (2)$$

where  $\mu$  is the medium viscosity,  $a$  the cell radius and  $G$  the shear rate. This yields a dragging force ranging between  $5 \times 10^{-8}$  and  $5 \times 10^{-7}$  N.

Now, a remarkable observation made in *in vivo* studies [123, 166] was that a notable proportion of granulocytes 'rolled' with a translation velocity ranging between 10 and about  $50 \mu\text{m}/\text{s}$ , i.e. about ten times lower than expected. This rolling phenomenon was inhibited by infusion of polyelectrolytes such as protamin and sulfated polysaccharides [166].

Recently, much information was obtained on this phenomenon by Lawrence and Springer who studied the movement of neutrophils subjected to a laminar shear flow along a surface coated with various amounts of purified ICAM and P-selectin molecules, acting respectively as ligands for the leukocyte  $\beta 2$ -integrins and LAM-1. This was done in a flow chamber allowing continuous monitoring of cell movement [111]. The translation velocity  $U$  of many leukocytes moving close to the wall was about  $500 \mu\text{m}/\text{s}$  when the wall shear rate was about  $250 \text{ s}^{-1}$ , corresponding to a ratio  $U/G_w a$  of about 0.5 (where  $a$  is the cell radius). This result may be compared to theoretical estimates obtained by Goldman et al. [78] who studied the movement of a neutrally buoyant sphere subjected to a laminar shear flow near a plane surface (fig. 4). The estimated value of  $U/G_w a$  varied between 0.68 and 0.45 when the ratio  $\delta/a$  between the cell-to-surface gap and the cell radius varied between 0.045 and 0.003 (i.e.  $0.18 \mu\text{m}$  and  $12 \text{ nm}$  for a cell of  $4 \mu\text{m}$  radius). Although the relevance of Goldman's results to the movement of actual cells may be questioned (see [170] for an experimental check of the theory), it may be concluded that the aforementioned velocity is indicative of a rather unconstrained motion.

Further, when the surface was coated with P-selectin, a proportion of cells exhibited much lower translational velocities of a few  $\mu\text{m}/\text{s}$ , with visible rolling. However, the P-selectin could not induce strong adhesion: if the flow was stopped and resumed several minutes later, cells started to roll again.

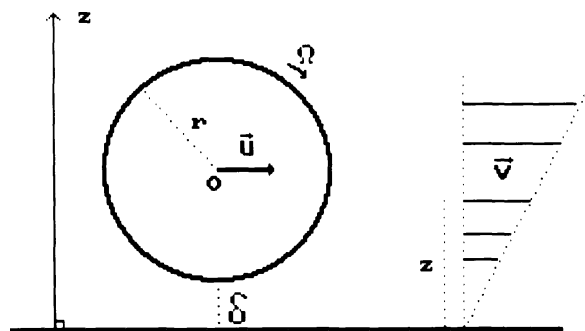


Fig. 4. Motion of a sphere subjected to a laminar shear flow near a plane surface. The motion of a neutrally buoyant sphere subjected to a laminar shear flow near a plane surface was determined by Goldman et al. [82]. The displacement is a combination of a translation with velocity  $U$  parallel to the wall and angular velocity  $\Omega$ . When the distance  $\delta$  between the sphere and the wall becomes small, the dimensionless ratios  $U/Gr$  and  $\Omega/G$  decrease very slowly, as  $1/\ln \delta$ .

In contrast with the above data, when activated leukocytes were driven along an ICAM-1-coated surface with substantial flow rate, no rolling nor attachment was observed. However, if cells were deposited on the same surface under static conditions, they readily spread within 5 minutes, and they remained bound when the flow was resumed. Finally, attachment under flow conditions could occur when the surface was coated with both ICAM-1 and P-selectin. Hence, selectins can induce rapid but transient adhesion, whereas integrins can form strong adhesions provided the interaction time is fairly long. Possible explanations for the different behavior of these molecular species will be discussed in section 4.

### 2.3. Interactions between cells and artificial surfaces

The increasing practice of cell culture was a strong incentive to study the mechanism of interaction between different cell populations and culture dishes (fig. 5). Also, the use of artificial polymers for medical purpose (e.g., as implants in dentistry or surgery, as contact lenses in ophthalmology, as dialysis membranes in nephrology) triggered strong interest for the relationship between the surface properties of polymers, cell adhesion and spreading. In the present section, we shall describe some basic data. Biophysical approaches relevant to these problems will be reviewed in section 4.

#### 2.3.1. Surface energy

Much experimental evidence suggests that nonspecific physical properties related to surface energy play an important role in the interactions between cells and polymer surfaces in a protein-free environment. We shall first recall some basic definitions [4, 24].

The surface energy  $\gamma$  of a homogeneous substance is simply the free energy increase associated to the formation of a free surface of unit area in vacuum. The interfacial energy  $\gamma_{12}$  between two media (1) and (2) is the free energy required to create an interface of unit area between both media. The work of adhesion between

Fig. 5. Cell adhesion to flat surface. Cells from the P388D1 murine macrophage-like cell line were deposited on a glass coverslip. A fluid phase fluorescentmaker (fluoresceinated dextran) was added in the bulk medium and cells were examined with a confocal laser scanning microscope, thus allowing direct visualization of sections perpendicular to the coverslips. Bar is 18  $\mu\text{m}$ .

media (1) and (2) is the work done by the system when two free surfaces of media (1) and (2) are brought into contact. Clearly,

$$W_{12} = \gamma_1 + \gamma_2 - \gamma_{12}. \quad (3)$$

Now, in situations of biological interest, adhesion is performed in aqueous solution (this is medium 3). The work of adhesion between two media (1) and (2) embedded in a third medium (3) is given by

$$W_{12}^3 = \gamma_{13} + \gamma_{23} - \gamma_{12}. \quad (4)$$

The surface energies of liquids and the free energies of liquid/liquid interfaces can be measured directly. However, direct experimental determination of the surface energies of solids is much more difficult to achieve. The most widely used procedure

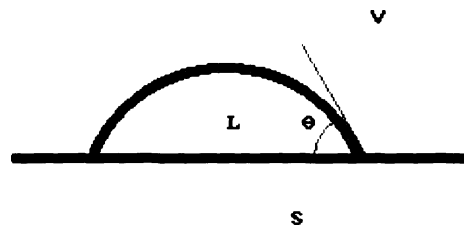


Fig. 6. Definition of contact angles. A droplet of a liquid L is deposited on a plane solid surface S. The third phase may be a vapor (V) or a liquid immiscible with L. Experimental determination of the contact angle  $\theta$  between the solid surface and a plane tangent to the upper droplet surface on the three-phase-line provides a relationship between the three interfacial energies (SL, SV and LV).

consists of measuring the contact angle of liquid droplets on solid surfaces (fig. 6) and using the Young–Dupré equations

$$\gamma_{LV} \cos \theta + \gamma_{LV} - \gamma_{SV} = 0. \quad (5)$$

Hence, only the difference ( $\gamma_{S1} - \gamma_{SV}$ ) can be measured. Much work was devoted to the derivation of ‘combining rules’ allowing determination of all parameters. Unfortunately, whereas this approach met with some success when polymers and simple organic liquids were considered, its relevance to biological systems is questionable due to the multiplicity of specific interactions that cannot be accounted for by these formulae (see section 4 for more details).

The simplest combination rule, that apply to series of apolar media, may be written as

$$\gamma_{12} = (\sqrt{\gamma_1} - \sqrt{\gamma_2})^2. \quad (6)$$

This formula is a consequence of the assumption that the work of adhesion between substances (1) and (2) is a product of material parameters characteristic of (1) and (2). See section 4.2.1.

Combining equations (6) and (3) yields the work of adhesion between two materials (1) and (2) embedded in medium (3):

$$W_{12}^3 = 2(\sqrt{\gamma_3} - \sqrt{\gamma_1})(\sqrt{\gamma_3} - \sqrt{\gamma_2}). \quad (7)$$

Thus, the work of adhesion will be positive (i.e. the media will stick together) unless  $\gamma_1 < \gamma_3 < \gamma_2$  or  $\gamma_2 < \gamma_3 < \gamma_1$ . If the surface energy  $\gamma_3$  of the bulk medium is equal to the surface energy of one of these substances (say 1), the work of adhesion will be zero, and thus will not depend on the surface tension of the other material.

Now, we shall review some experimental data: a very interesting series of experiments were performed by Van Oss and coworkers [138] who studied the adhesion of blood neutrophils and platelets to a series of polymer surfaces (the contact angle of water on these surfaces varied between 110 and 24 degrees). The medium was a saline solution supplemented with various amounts of dimethyl sulfoxide with a surface free energy ranging between 63.2 and 72.8 mJ/m<sup>2</sup> (15% and 0% dimethyl sulfoxide respectively). In accordance with simple theoretical predictions, adhesion was respectively increasing, constant or decreasing when the substrate surface energy was increased if the medium surface energy was respectively lower than, equal to or higher than the estimated free energy of the cell surface. Similar results were obtained when glutaraldehyde-treated erythrocytes were used as test particles [3]. The influence of the substrate free energy on the adhesion and spreading of different cell lines was later confirmed by other authors [151].

However, the above studies revealed that cell adhesion occurred when the estimated work of adhesion was zero, which suggested that other unaccounted interactions might play a role in cell-substrate binding [3].

### 2.3.2. Surface charge

It has long been shown with electrophoretic measurements that mammalian cells bear a net negative charge [133]. Electrostatic repulsion may thus in principle inhibit adhesion between cells and negative surfaces. For the sake of clarity, quantitative calculations will be described in section 4, and we shall now review some notable experimental results.

First, it was unambiguously demonstrated that cell-cell or cell-surface adhesion could be efficiently inhibited by electrostatic repulsion in solutions of low ionic strength (say 1 mM NaCl or less). This was shown in very elegant experiments by Gingell and Todd who studied the equilibrium position of glutaraldehyde-treated erythrocytes sedimenting on a charged oil-saline interface [81]: at low ionic strength, red cells remained about 100 nm above the interface, which would have efficiently prevented the formation of specific bonds.

However, in physiological media (i.e. about 150 mM NaCl and a few mM divalent cations), electrostatic repulsion between charged surfaces is screened by counterions with an exponential decay of characteristic length close to 0.8 nm (this is the Debye-Hückel length). It is therefore of interest to consider experiments performed at physiological ionic concentration. Sugimoto [163] studied the behavior of fibroblasts deposited on two different surfaces: glutaraldehyde-polymerized bovine albumine had a high negative charge. When polylysine was added to the polymerizing mixture, the surface charge was decreased by more than 50% as assessed by electrophoretic mobility determinations. When cells were deposited on the less negative substrate, they flattened and became immobile. Electron microscopical studies revealed much tighter apposition between cell and substrate surfaces when polylysine was added.

Similar results were obtained in a study made on the interaction between rat macrophages and sheep erythrocytes that had been made hydrophobic by glutaraldehyde treatment: the negative charge of these erythrocytes was decreased either by coating them with positively charged polylysine molecules or by removing negative sialic acid groups by neuraminidase treatment. In both cases, the efficiency of macrophage-particle adhesion was dramatically increased [30], and electron microscopy revealed tighter apposition between macrophage and erythrocyte surfaces when the negative charge was decreased [29, 129]. Concordant conclusions were obtained by Rutishauser and colleagues who studied the tightness of apposition between neural cells bound by intact or desialylated Neural Cell Adhesion Molecules [149].

Electrostatic repulsion may thus modulate the tightness of cell-cell or cell-substrate adhesion.

### 2.3.3. Other cell surface properties

Margolis and colleagues studied the adhesion of mouse fibroblasts to lipid films adsorbed on glass surfaces [120, 121]: Adherence was better with gel-crystalline than with fluid phases. In other experiments performed by Springer and colleagues, lymphocytes were deposited on solid surfaces coated with adhesion molecules (LFA-3 or ICAM) that were either immobile or free to diffuse: similar spreading was obtained in both cases [32].

#### 2.3.4. *Macromolecule adsorption*

An important point concerning the interpretation of experimental data is that solid surfaces exposed to serum-containing media will rapidly become coated by a layer of adsorbed molecules [13]. This possibility cannot be ruled out when experiments are conducted in protein-free solution, since most cells constitutively release diverse macromolecules that can serve as intermediates for substrate adhesion. As an example, fibroblasts secrete fibronectin, a protein made of two subunits of 250,000 molecular weight that possesses multiple binding sites and readily adheres to polymer surfaces [87] as well as specialized membrane receptors on the fibroblast (see [40] for more details on these molecules). Similarly, glycosaminoglycans such as hyaluronic acid or chondroitin sulphate may mediate cell adhesion [155] by adhering to both cell membranes and culture surfaces.

Clearly, the physiological importance of the intrinsic physico-chemical properties of substrates might be questioned if they are coated with a layer of biological macromolecules in all physiologically relevant conditions. However, two points must be noticed. First, the properties of tested surfaces may influence the nature of adsorbed molecules by influencing the competition between solute substances [2, 41]. Secondly, adsorbed proteins may exhibit conformational changes that may depend on the substrate properties [159]. Indeed, several authors suggested that the surface structure of adsorbed molecules might reflect the nature of the underlying substrate [2, 151].

#### 2.3.5. *Mechanical properties of cell-substrate adhesion*

Many authors attempted to measure the mechanical strength of cell-substrate adhesion. We shall present some representative results.

The micromanipulation approach consisted of detaching adherent cells with a flexible micropipette. Suitable calibration allowed quantitative derivation of the applied force from the pipette curvature as measured immediately before detachment. This procedure was recently used by Gingell and colleagues [78] who measured at the same time the strength of adhesion and the area of tight apposition between cells and substrate (they made use of interference reflection microscopy). The strength of adhesion between *Dictyostelium discoideum* and an hydrophobic substrate (silanized glass) was of the order of 10 nanonewton, with a close contact area of 1–4  $\mu\text{m}^2$ . In other experiments, McKeever used the same approach to measure the strength of adhesion between macrophages and glass surfaces: the reported value was about 100 nanonewton [125].

Following another approach, Bongrand and colleagues deposited adherent cells in glass capillary tubes. After a suitable adhesion time, cells were subjected to hydrodynamic flows of increasing strength. In some cases, viscous dextran solution had to be used in order to ensure that the flow be laminar. The main conclusions were as follows:

- i) the minimal flow rate required to detach cells was dependent on the duration of force application.
- ii) A tangential force on the order of 50 nanonewton per cell was required to separate macrophage-like P388D1 cells from glass surfaces [128], similar

values were obtained when blood granulocytes were separated from glass surfaces coated with various molecular species such as albumin, fibronectin, concanavalin A or polylysine [127] and human melanoma cells were detached from fibronectin-coated glass surfaces [8].

A third approach consisted of subjecting adherent cells to a centrifugal force. Easty and colleagues could separate murine tumor cells from glass substrates with a centrifugal acceleration in the order of  $1,000\times g$  parallel to the substrate plane. The corresponding force was thus about 0.1 nN [57]. Corri and Defendi centrifuged glass surfaces bearing adherent macrophages or red cells. The minimal force required to break cell substrate adhesion was 56 nanonewton for macrophages and less than 0.1 nanonewton for erythrocytes [37]. Interestingly, the authors noted that the minimal separating force was decreasing when the duration of application was increased. Using a similar experimental setup, McClay and colleagues [124] found that adhesions between chick embryo cells could be ruptured by a force of about 0.1 nN. However, when these cells were deposited on polylysine-coated surfaces, they resisted a centrifugal acceleration of  $3,000\times g$ , corresponding to a force higher than 3 nN.

In conclusion, we described three general models of cell adhesion in order to help the reader evaluate the significance of the problems discussed below. These examples showed that biological adhesion is mediated by an impressive number of ligand molecules and that binding may be modulated by nonspecific physical interactions.

### 3. Biophysical characterization of cells

The first step to a biophysical modeling of cell adhesion is to build a quantitative description of the cell features likely to play a role in this process. This goal is made difficult by the diversity of living cells: If we consider only a single cell type, the interest of our description will be restricted by the difficulty of assessing its relevance to other models. On the other hand, gathering conclusions from studies performed with widely different cell species is not warranted. Therefore, we shall try to keep an intermediate way: we shall essentially refer to leukocytes (i.e. lymphocytes, monocytes and granulocytes) that are ideally suited to studies done at the individual cell level. Occasional data concerning other cell populations will also be provided for comparison.

We shall sequentially consider three different scales: first, the micrometer scale, i.e. general cell shape control as studied with conventional optical microscopy. Secondly, the submicrometer scale, as observed with electron microscopy, since an important step of cell adhesion is the tight apposition of binding surfaces in order to allow molecular bonding. Finally, we shall describe the molecular organization of the cell surface, with an attempt to describe general physical properties without delving into a description of individual molecular species. Clearly, present knowledge does not allow the derivation of quantitative relationships between the three organization levels we mentioned.

### 3.1. Cell shape control

Many cell types are fairly spherical when they are maintained in suspension under resting conditions (however, some cell populations may display micrometer-sized protuberances that cannot be neglected, see, e.g., [170]). Spontaneous deformations can be induced by biochemical stimuli in absence of any adhesive interaction. Thus, exposing suspended neutrophils to chemotactic factors such as formyl methionyl peptides will induce spectacular cell polarization within a few minutes (fig. 7).

Now, if a rounded cell is deposited on a substrate, it will exhibit some kind of flattening (fig. 5). This deformation may involve several mechanisms. First, the cell may flatten under the mere influence of gravity. Secondly, adhesive cell-substrate interactions may act as a tensile force triggering cell spreading with strong analogy to the spreading of a liquid droplet on a solid surface as a consequence of the balance between interfacial forces. Thirdly, the cell may send active lamellipodia that will be secondarily bound by the substrate. Since adhesive interactions may deliver activating signals, it is very difficult to discriminate between these mechanisms [43]. However, it may be useful to estimate the minimal force required to deform a cell in absence of known activation, since such deformation may be a prerequisite to adhesion in some circumstances.

Many procedures were used to study bulk cell deformability, including centrifugation on a surface with measurement of induced deformation [94, 131], determination of the resistance to indentation with a moving stylus [141, 142] or aspiration into a glass micropipette. The latter method was probably the most widely used during the last ten years and provided a wealth of information of granulocyte deformability. The main conclusions are as follows. When a typical granulocyte of about  $4\ \mu\text{m}$  diameter is sucked into a pipette of, e.g.,  $2\text{--}3\ \mu\text{m}$  diameter with a pressure higher than some threshold value [67], it forms a protrusion that will enter the pipette and grow with a velocity depending of the pressure and pipette size. If the pipette is large enough (e.g.,  $4\ \mu\text{m}$  diameter), the cell will readily acquire a sausage-shape and flow into the pipette. If the pipette diameter is smaller, the deformation will be limited by a maximum extension of the apparent membrane area that may increase by a factor of about two [72]. If the pressure is reversed, the cell will be expelled and it will resume its spherical shape within several tens of seconds ([164], see fig. 8). All authors observed both viscous and elastic behavior, and several quantitative models were elaborated to account for measured deformations. In a remarkable work, Schmid-Schönbein and colleagues [154] studied the small deformations induced within a few seconds by moderate aspiration. They modeled cells as homogeneous standard viscoelastic solids (fig. 9) and readily solved the equations of deformations. They were thus able to derive three material constants: the elastic stiffness coefficients  $k_1 = 275\ \text{dyn/cm}^2$ ,  $k_2 = 737\ \text{dyn/cm}^2$  and a viscosity coefficient  $\mu = 130\ \text{dyn}\cdot\text{s/cm}^2$ . In another series of experiments, Evans studied large granulocytes deformations [67] and results were consistent with the model of a tensile surface (about  $0.01\ \text{dyn/cm}$  tension) surrounding a highly viscous fluid (a later figure for the viscosity was about  $1,000\ \text{dyn}\cdot\text{s/cm}^2$  [72]). Later reports led the authors to propose more sophisticated models, with a combination of a stressed surface and visco-elastic interior, in order

Fig. 7. Cell shape control. Human granulocytes were fixed and labelled with a fluorescent phalloidin derivative to reveal actin microfilaments. They were then studied with confocal laser scanning microscopy and series of 16 sections separated by a distance of  $1\ \mu\text{m}$  are shown. A: resting cell maintained in suspension. It is spherical. B: cell pretreated with a chemoattractant for 15 minutes. It exhibits marked polarization with a microfilament concentration at the cell leading edge. Bar is  $18\ \mu\text{m}$ .

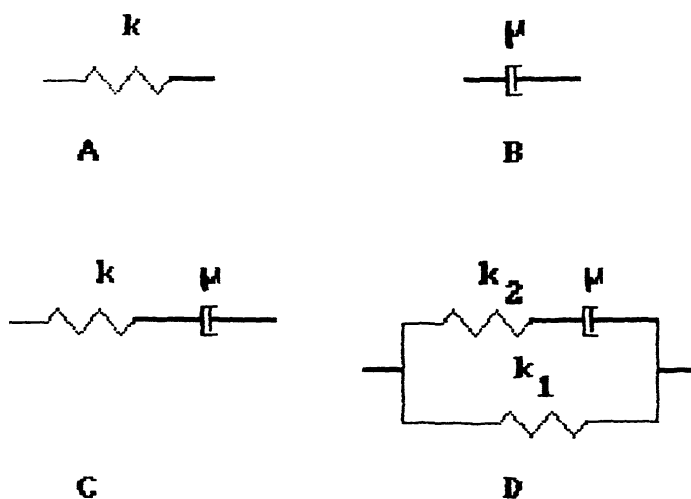


Fig. 8. Simple models to represent cell mechanical properties. The following mechanical model may be considered to represent the properties of a volume element of a solid body. (A) elastic medium with spring constant  $k$ . The force  $F$  is proportional to displacement  $(x - x_0)$ , where  $x_0$  is the unperturbed length. (B) viscous medium, the force is proportional to the rate of deformation  $dx/dt$ . (C) Maxwell solid. (D) Standard viscoelastic medium.

Fig. 9. Cell shape recovery after micropipette aspiration. A murine macrophage-like P388D1 cell was sucked into a micropipette, then expelled and observed while it recovered its spherical shape. It is shown 0 s (A), 5 s (B), 11 s (C) and 16 s (D) after expulsion. Bar is  $4 \mu\text{m}$ .

to account for mechanical cell behavior during aspiration and shape recovery [56, 164, 173].

Since a more complete discussion of cell shape control would not fall into the scope of the present review, we shall add only a few points.

Whereas proposed models may satisfactorily account for cell deformations caused by a restricted range of applied force intensity and duration, it may be dangerous to use material parameters to predict cell behavior under conditions widely different from those used to derive these parameters.

It was often stressed that individual cells might display quite diverse behavior. Indeed, studying single cells makes apparent the danger of considering only mean values determined on cell populations.

Many different cell species were studied with the micropipette aspiration technique. In the author's laboratory, rat macrophages [129], macrophage-like [131] or lymphoid [76, 131] and basophilic [96] cell lines and human melanoma cells [8] were studied with this technique. An important conclusion is that very marked differences may be found between cells in an apparently homogeneous cell population.

Interestingly, the spontaneous traction exerted on their substrate by epithelial cells was quantified: fibroblasts deposited on an elastic surface exerted a constant traction on the order of 0.001 dyne/cm along the advancing margin [89]. More recently, the contractile force of fibroblasts and endothelial cells was estimated at  $4.5 \times 10^4$  and  $6 \times 10^4$  dyne/cm<sup>2</sup> respectively (i.e. on the order of 0.045–0.06 dyne/cm on the cell margin, assuming a cell thickness on the order of 1  $\mu\text{m}$  [106]). These estimates are fairly close to the values reported for neutrophils, and may represent a minimum order of magnitude for the adhesive energy required to induce the formation of a substantial contact area between a cell and an adhesive substrate in absence of active deformation.

A final point of interest is the mechanical strength of cell membranes. Although marked differences are found between tested cell populations, following our experience, membrane rupture is not an uncommon event when cells of 4–7  $\mu\text{m}$  diameter are subjected to a sucking pressure of 25 cm H<sub>2</sub>O with a pipette of 2–3  $\mu\text{m}$  inside diameter (see, e.g., [8]). The corresponding tension is about 2 dyne/cm. Obviously, the membrane resistance sets a limit to the strength of cell-cell and cell-surface adhesion.

### *3.2. Cell surface roughness: the submicrometer scale*

The interpretation of quantitative data on cell contact formation and binding strength is crucially dependent on the actual area of membrane regions involved in adhesion [88]. Further, the electron microscopic study of cell surfaces reveals the presence of numerous protrusions of variable size that are often inapparent when cells are observed with conventional microscopy. Finally, when contact areas between adherent cells are studied with electron microscopy [76, 129] it often appears that the distance

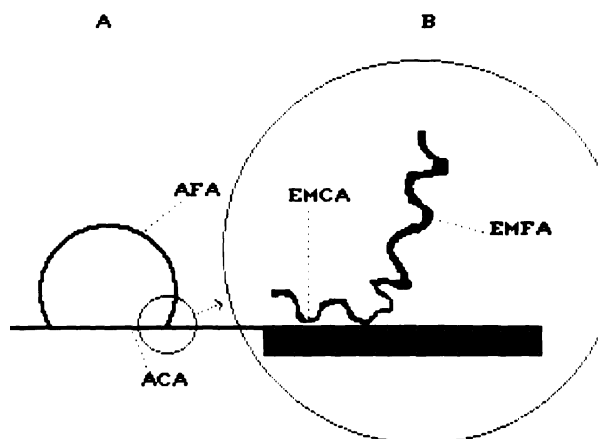


Fig. 10. Apparent and actual adhesion areas. Figure A represents a typical substrate-bound cell depicted with the resolution of conventional optical microscopy. The apparent free area (AFA) is the area of a portion of a sphere and the apparent contact area (ACA) is a disc. Figure B represents a portion of the figure depicted with the resolution of electron microscopy. The electron microscopic free area (EMFA) is larger than the apparent free area due to the presence of numerous cell surface asperities. In the apparent contact area, only a fraction of the cell membrane is separated from the surface by a gap compatible with molecular bonding. This defines the electron microscopic contact area (EMCA). It is not easy to determine whether the whole EMCA is involved in binding. Figure C represents a binarized image of an electron micrograph representing a portion of the interaction area between concanavalin-A-agglutinated rat thymocytes [31]. Bar is  $0.1 \mu\text{m}$ .

between the phospholipid bilayers of the plasma membranes is very irregular, with

a combination of zones of apparent molecular contact (the distance between bilayers is in the order of 20–40 nm) and regions where membranes are separated by a gap of several hundreds of nanometers that is obviously incompatible with adhesion between membrane intrinsic receptors (see next section).

In order to clarify this point, it is important to give a precise definition of the parameters we are studying (fig. 10): First, the *apparent cell area* may be defined as the area of a smoothed cell where only details visible with optical microscopy are retained. This area is simply  $4\pi R^2$  for a spherical cell of radius  $R$ . Second, the *actual membrane area* is the bilayer area. This may be derived from quantitative processing of electron microscopical images, using basic formulae of stereology [61]. Similarly, the *apparent binding area* is the area of the region where cells appear bound when studied with optical microscopy. The *electron microscopic binding area* is the area of the region where the intermembrane distance is compatible with molecular adhesion. This last definition requires several points of caution. First, it is not proven that there are actual molecular bonds in a region where the intermembrane distance is consistent with bonding. Secondly, since the relative orientation of a microscopic section plane and interacting membranes is random, the apparent intermembrane distance as estimated on micrographs is expected to be higher than the actual distance (it may be shown that the mean apparent distance is about twice the actual distance [76]). Thirdly, it is difficult to assess the influence of sample processing for electron microscopy on intermembrane distance.

We shall now describe some experimental data relevant to the control of cell roughness.

An important result emerging from numerous observations made on living cells is that they deform with constant volume, variable *apparent area* and constant *actual membrane area*. Indeed, it has long been demonstrated that erythrocytes deformed with essentially constant area, since membrane rupture occurred after a few percent relative area increase [71]. Further, the observation of the deformation of mesenchyme cells suggested that the formation of a protrusion inhibited the appearance of other protrusions, due to a mechanical resistance of the membrane [184]. Also, electron microscopic studies confirmed that microvilli and blebs acted as reserve surface membrane [63]. It was estimated that the actual membrane area of mastocytoma cells was between 50% and 100% higher than the apparent area [105]. The excess area of blood cells compared to spheres of equal volume was reported to range between 44% and 130% [34]. These estimates were fairly consistent with the report that the maximal apparent area increase of blood granulocytes sucked into micropipettes was in the order 110–120%, supposedly corresponding to full membrane extension [72].

The size of cell surface asperities may be readily estimated from electron micrographs: the length of protrusions was 0.4–0.5  $\mu\text{m}$  in mastocytoma cells [105] and kidney fibroblasts [63]. Values as high as 2  $\mu\text{m}$  were found on a T-cell hybridoma with particularly large protrusions that appeared in optical microscopy [170]. This must be considered as a maximum value. The thickness of protrusions was about 0.1  $\mu\text{m}$  in aforementioned studies. These values seem representative of images found on many cell types.

An important point is that cell surface protrusions may resemble sheets or cylinders, depending on cell type, with similar appearance on transmission micrographs. Scanning electron microscopy may be useful to derive the three-dimensional cell shape.

An important problem is to determine the mechanical properties of cell surface asperities: micropipette aspiration studies cannot tell us whether the cell membrane must be viewed as a flaccid surface subtended by the subplasmalemmal cytoskeletal network, or whether each asperity is endowed with mechanical resistance and individually resists smoothing (as was assumed in [129]). Indirect evidence is provided by immunofluorescence studies: cell protrusions were demonstrated to contain actin as well as cytoskeletal and membrane binding structures such as vinculin, talin,  $\alpha$ -actinin and filamin [45]. Hence it seems reasonable to ascribe these asperities material parameters similar to those derived for bulk cells. However, more precise studies are needed to understand the behavior of these asperities during the first steps of contact formation.

### 3.3. Relevance of the concept of surface tension to biological membranes

The concept of surface tension proved very useful to relate the adhesion-induced deformations of liquid droplets or lipid vesicles to interaction energies [4, 69]. It is thus warranted to ask whether this can be applied to nucleated cells such as leukocytes.

An important difficulty is that there is no rigorous experimental means of discriminating between the membrane and cytoplasm resistance to deformation. Therefore, the derivation of a surface tension from deformation measurements requires some assumptions concerning the mechanical properties of the cell interior. The experimental observation that many cells

- i) are spherical in suspension, and
- ii) recover to the spherical shape after deformation (figs 7, 8) strongly supports the proposal by Evans [67] that the mechanical properties of blood granulocytes might be accounted for by the model of a highly viscous liquid surrounded by a tensile membrane.

According to this concept, the relationship between the *effective membrane tension* and apparent cell area increase might be derived from the *equilibrium value* of the length of protrusions obtained by sucking cells into micropipettes with varying pressure. The finding by Evans that granulocytes entirely penetrated through a pipette when the suction pressure was higher than a threshold level inversely related to the pipette diameter and required to obtain the formation of a spherical protrusion strongly suggested that the tension was fairly constant (provided the membrane was not fully extended). This tension ranged between 0.01 and 0.035 dyne/cm. However, when macrophages, activated lymphocytes or melanoma cells were subjected to micropipette aspiration, the growth of the cell protrusion often stopped before complete cell entry into the pipette. It is not clear whether this arrest was due to an actual increase of membrane tension concomitant with apparent area increase, or a blockade when the cell nucleus or some other cytoplasmic structure entered the

pipette tip (this point is emphasized in ref. [8] see also fig. 12). This may impair the significance of empirical relationships obtained between apparent surface tension and apparent membrane area increase [76, 129].

Further, the concept of membrane tension is useless at the electron microscopical level. If we assume that the plasma membrane is a folded sheet of low mechanical resistance deposited on an underlying 'contractile carpet' [67], the thermodynamic cost of creating a *small* contact region with a smooth surface will be zero for a leukocyte, in contrast to an erythrocyte that exhibits an intrinsic biconcave shape. This difference may account for the well known difficulty to make erythrocytes stick to rigid surfaces as compared to other cell types.

Another possibility would be that the polymorphism of membrane lipids in leukocytes might favor the occurrence of a variety of microdomains with different curvatures, allowing each lipid molecule to find an ideally suited environment. In this case, a folded appearance would be favored. Clearly, more work is required before we understand the mechanisms responsible for cell surface roughness at the micrometer and submicrometer level.

### 3.4. Molecular structure of the cell surface

We shall only review some peculiar properties with an obvious relevance to cell adhesion. The point we wish to address may be summarized as follows: suppose the distance between two cells is gradually decreased. It is probable that they will first exert some mutual repulsion (otherwise, spontaneous agglutination would occur in absence of any specific bonding). The force/distance law characterizing this repulsion must depend on many parameters, including the density of charges and membrane-bound stabilizing polymers, and the mobility of these molecules. Indeed, if contact is made slow enough, repulsive molecules are expected to depart from the contact region or gather into restricted areas, as predicted in view of theoretical considerations [16] and suggested by electron microscopical evidence [149].

The following data may be of interest in this respect.

#### 3.4.1. Bulk composition of plasma membranes

Estimates for mean membrane composition were suggested in previous reviews [7, 23, 24]. More details can be found in standard textbooks on cell membranes [80]. The basic structure of the plasma membrane is a phospholipid bilayer where intrinsic glycoproteins and glycolipids are embedded. A reasonable order of magnitude for the composition is 45% protein / 45% lipid / 10% carbohydrate. Assuming a mean phospholipid/cholesterol ratio of 0.72, the mean area for (1 phospholipid + 0.72 cholesterol) is  $0.77 \text{ nm}^2$  [114], corresponding to a molecular weight of about 1,000. Modeling proteins as globular units of 4 nm diameter and 50,000 molecular weight, the occupied area is about  $2.75 \times 10^9 \text{ cm}^2$  per gram (i.e. 0.45 g protein and 0.45 g lipid), with 25% of the total area occupied by proteins.

Another estimate may be useful: assuming that water represents about 70% of the mass of a standard cell [113], the dry mass of a typical leucocyte of  $4 \mu\text{m}$  radius and  $1.077 \text{ g/cm}^3$  density is about  $8.7 \times 10^{-11} \text{ g}$ , with a corresponding membrane area of  $400 \mu\text{m}^2$  (i.e. twice the apparent area). The plasma membrane therefore represents 1–2/100,000 of the total cell dry weight.

### 3.4.2. *Intrinsic membrane glycoproteins*

Since many adhesion receptors are intrinsic membrane proteins, it is important to have a general feeling of their shape and flexibility. Members of the immunoglobulin superfamily are an important example of such proteins. They are made of one or several domains of about  $2.5 \times 2.5 \times 4$  nm, with fairly high rigidity and bound by structures of variable flexibility. Thus, surface immunoglobulin G found on B lymphocytes may protrude by about 10 nm above the bilayer, with easy rotation of the external antigen binding sites [175]. Class I major histocompatibility complex molecules that are found on nearly all cell species have a similar size (with a 3-domain chain associated to  $\beta$ 2-microglobulin). ICAM-1 molecules, that have an obvious adhesive function, are made of two seemingly rigid rods of 11.8 and 6.9 nm length separated by a fairly flexible region [161]. Human fibronectin receptors were described as intrinsic membrane proteins with an extracellular region of 12–14 nm length. Hence, intrinsic membrane proteins may be viewed as structures of 10–20 nm length with limited flexibility.

### 3.4.3. *The glycocalyx*

Electron microscopic studies have long revealed that in nearly all tested cells the phospholipid bilayer of the plasma membrane was coated with a low density region of varying depth [178], ranging between a few tens and several hundreds of nanometers [122, 178, 187]. This ‘fuzzy coat’, or ‘glycocalyx’ was first revealed by the occurrence of a gap between plasma membranes in contact regions between adherent cells [122]. This was later reported to be stained with various procedures such as periodic acid Schiff (PAS), phosphotungstic acid (PTA), Colloidal iron or thorium, ruthenium red, alcian blue, and it was suggested that this region had relatively high polysaccharide content. Other biochemical studies showed that most membrane carbohydrates were oligosaccharidic chains bound to glycoproteins or glycolipids. They are made of less than eight [36] to 20 [178] monosaccharide units, corresponding to an extended length lower than 5–10 nm.

Thus, the structure extending outside the 20 nm region next to the phospholipid bilayer represents a minimal fraction per weight of the membrane. It includes glycosaminoglycans that are made of repetitive monosaccharide units: hyaluronic acid is made of several thousands repeats of a characteristic disaccharide sequence (N-acetyl glucosamine  $\beta$ 1–4 glucuronic acid) $\beta$ 1–3. Similarly, chondroitin sulfate is made of hundreds of units [108]. These chains are relatively unbranched [10]. Since their conformation may play an essential role in adhesion, we give some basic results and refer the reader to more complete references for additional details [10].

The conformation of long flexible polymer chains received much attention, and basic ideas are described in the classical book by Flory [75]. This conformation is essentially dependent on the interaction between the solvent and repeating units. If there is no free energy variation associated to the transfer of monomers into solvent (this is the case for so-called  $\theta$  solvent conditions), the chain conformation is well approximated by classical random walk models, and the end-to-end distance is proportional to the square root of the number  $N$  of monomer units. Now, if the transfer of monomer units into solvent results in a net free energy decrease, the net

repulsion between the monomers will provoke a relative expansion of the chain, and the molecular size will increase as a power of  $N$  that will be higher than 0.5. This property can be used to study polymer conformation by measuring the viscosity of dilute polymer solutions. The starting point is Einstein's formula that states that the viscosity  $\mu$  of a suspension of rigid spheres is

$$\mu = \mu_0(1 + 2.5\Phi) \quad (8)$$

where  $\mu_0$  is the viscosity of the pure solvent and  $\Phi$  is the fraction of the total volume occupied by the spheres [60]. It may be shown that individual polymer molecules behave like hard spheres. Thus, defining the intrinsic viscosity as

$$\mu_{\text{sp}} = \lim_{c \rightarrow 0} (\mu - \mu_0) / \mu_0 c \quad (9)$$

where  $\mu$  and  $\mu_0$  are the viscosities of the polymer solution (of concentration  $c$  expressed in  $g/dl$ ) and pure solvent respectively, it is found that this parameter is related to the molecular size of polymers following the empirical Mark–Houwink formula

$$\mu_{\text{sp}} = KM^\alpha \quad (10)$$

where  $M$  is the polymer molecular weight, and  $\alpha$  is an empirical coefficient that is close to 0.5 in a  $\theta$  solvent and is expected to be higher than 0.8 if the polymer is rigid and rod-like rather than coiled.

The Mark–Houwink coefficient was about 0.8 for hyaluronate and was sometimes higher than 1 for chondroitin sulfate [10]. It is concluded that water is probably a good solvent for polysaccharides constituting the cell coat. This point is of importance if we wish to predict intercellular forces during cell-to-cell approach.

Another point of interest is the mode of attachment of glycosaminoglycans to the cell surface. They may be bound to core proteins, forming proteoglycans [189]. These proteins may be inserted in the membrane with a transmembrane and intracellular regions, or covalently bound to a phosphatidyl inositol group. Also, glycosaminoglycans can interact with other elements of the pericellular matrix [91, 189]. Thus, fibronectin binds to heparin [136]. Also, the CD44 membrane protein has an affinity for hyaluronic acid [90]. Interactions between glycosaminoglycans were also described [10]. In conclusion, glycosaminoglycans may be viewed as long unbranched chains firmly anchored to plasma membranes with multiple low affinity binding sites to these membranes. Functional interactions were also reported between proteoglycans and submembranar cytoskeletal elements [188].

An important point is the concentration of these sugars in the pericellular matrix: this is difficult to quantify since the cell coat may be partially removed by rather mild procedures such as washing in denaturing medium [44] or possibly in physiological solutions [33]. Taniguchi and colleagues assayed leukocyte associated glycosaminoglycans [167]: they found 36  $\mu g$  uronic acid per 100 ml blood. Estimating blood leukocyte concentration at  $6 \times 10^8$ /ml with 400  $\mu m^2$  actual membrane area per cell,

Table 2  
Some physical properties of a standard cell.

Parameter	Order of magnitude
Radius (sphere)	4 $\mu\text{m}$
Density	1.077
Apparent membrane area	200 $\mu\text{m}^2$
Actual membrane area	400 $\mu\text{m}^2$
Length of microvilli	0.5–2 $\mu\text{m}$
Thickness of microvilli	0.1 $\mu\text{m}$
Electric charge	-0.024 Coulomb/m <sup>2</sup>
Membrane tension (at rest – ref. [67])	$\leq 0.02$ mN/m
Membrane tension (10–20% apparent area increase – ref. [129])	1 mN/m
Glycocalyx thickness	50 nm
monosaccharide density in external glycocalyx zone	0.5 residue/nm <sup>2</sup>

Some parameters relevant to cell-cell adhesion were evaluated to allow a quantitative assessment of different forces likely to influence initial contact. Note that the estimates for surface tension are heavily dependent on the choice of a mechanical model to interpret experimental data (see 3.3).

the uronic acid concentration would be about 0.5 monomer/nm<sup>2</sup>. In another study, the concentration of uronic acids and hexosamines were 23.5 and 20.4 nmole per 10 mg dry weight of SV40-transformed green monkey kidney cells [119]. Using a tentative estimate of  $2 \times 10^{-13}$  g per  $\mu\text{m}^2$  membrane area, we obtain about 0.5 monomer per nm<sup>2</sup>, in accordance with the aforementioned estimate. We assumed that essentially all assayed molecules were localized on the cell surface, which is supported by the finding that most cell sulfated proteoglycans may be removed by proteolytic treatment [147].

Other components of the cell coat are proteins such as fibronectin or laminin. The fibronectin molecules is made of two strands of 61 nm length, bound at their ends with a fixed angles. They display limited flexibility with three preferential bending sites [62]. More than 100,000 fibronectin molecules were reported to be bound by fibroblasts with an affinity constant of  $3.6 \times 10^{-8}$  M [126]. The binding of such molecules to the cell surface may involve multiple low affinity binding sites since this was competitively inhibited with the Arg-Gly-Asp-Ser (RGDS) tetrapeptide that displayed an apparent affinity constant of  $6 \times 10^{-4}$  M for their binding site [144]. These figures may be useful since the RGDS sequence is involved in many adhesive interactions.

Laminin is also a component of the extracellular matrix that may bind to the cell surface. It appears as made of three short rods (36 nm length) and one long arm (77 nm) of limited flexibility bound on one end [62]. The above estimates are summarized in table 2.

#### 3.4.4. Static distribution and mobility of membrane molecules

Cell cell adhesion is expected to depend i) on the nature of cell surface molecules

that will first meet when two cells collide each other, and ii) the possibility that adhesive molecules get matched and concentrated in contact areas.

We shall first consider the static distribution of membrane molecules. We shall not describe the polarization of some cell populations that grow in an anisotropic environment (e.g., thyroid cells with apical and basal sides). Although the membrane molecules of suspended leucocytes are often considered as randomly distributed, some reports suggest that it may not be the case. Thus, Abbas and colleagues [1] analyzed the distribution of surface immunoglobulins on murine B lymphocytes and found that it was non-random to a high degree of statistical significance, with small clusters and patterns of interconnecting networks. Many authors compared the density of potentially adhesive molecules on microvilli and flat membrane areas. Concanavalin A, a lectin with a specificity for  $\alpha$ -methyl mannose, was uniformly distributed on rat lymphocytes [183]. Similarly, membrane immunoglobulins were uniformly distributed on murine lymphocytes [115] but they were concentrated on the microvilli of ATP-depleted murine spleen cells [50]. More recently, the L-selectin adhesion molecule was found to be concentrated on the tip of neutrophil microvilli [143]. Interestingly, the activation of human neutrophils with phorbol esters concomitantly induced spontaneous clustering and functional activation of complement receptors [52]. Finally, a point that may be of interest is that a local concentration increase of acetylcholine receptors induced their aggregation on muscle cells [162]. These data strongly support the view that at least some membrane molecules are non-randomly distributed, and that this may influence adhesion.

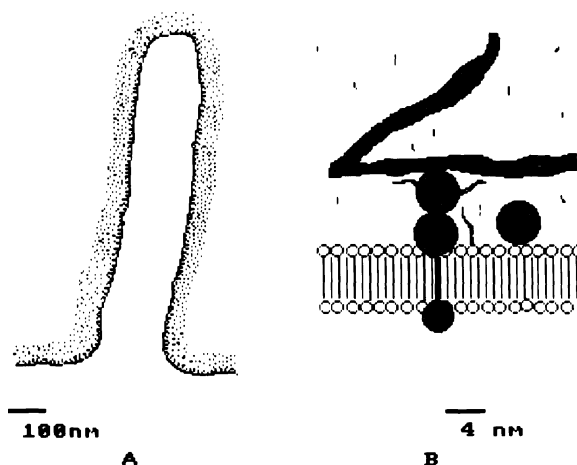


Fig. 11. The cell surface. The cell surface is represented on the left (A) with submicrometer resolution. A typical microvillus of  $0.1 \mu\text{m}$  thickness is studded with intrinsic membrane proteins. The monosaccharides of the cell glycoalyx are represented as individual points with realistic density. However, these points are much larger than individual hexasaccharides: otherwise, they would not be visible. Figure B represents a region of the cell surface with molecular resolution. The large V-shaped extracellular structure might represent a part of a fibronectin molecule (no fibronectin receptor is shown). Glycoalyx structures are represented with fairly realistic size and density. They are parts of long chains that intersect the plane of the drawing.

The mobility of membrane molecules received much attention. The most popular method of studying molecular movements is probably based on fluorescence recovery after photobleaching (FRAP; [152]). Briefly, a population of membrane molecules are tagged with fluorescent groups and the beam of a laser matching the excitation wavelength of the fluorophore is focused on a limited area (in the order of  $1 \mu\text{m}^2$ ) of the cell surface. The laser power is transiently increased in order to bleach fluorescent groups. The same area is then illuminated with lower intensity, and the variations of fluorescence are recorded. It is thus possible to derive the diffusion coefficient of fluorescent groups, and the fraction of mobile molecules in this population. The diffusion coefficient of several membrane molecules on lymphocytes (surface immunoglobulin or Thy1 molecule) was in the order of  $3 \times 10^{-10} \text{ cm}^2/\text{s}$  with a proportion of mobile molecules ranging between 50% and 90%. This value, which is representative of experimental data obtained on many proteins, was claimed to be about tenfold lower than the hydrodynamic limit [168], and the diffusion coefficient of membrane molecules was increased in 'blebs' induced on the membrane of muscle cells or on spectrin-depleted erythrocytes [107], thus strongly suggesting that the mobility of cell surface molecules was essentially limited by lateral constraints and interactions with submembranar cytoskeletal elements. This hypothesis was later tested by comparing the diffusion coefficient of wild-type molecules and engineered molecules with substantial deletions of intracytoplasmic domains: surprisingly, similar diffusion coefficients were obtained for normal and deleted class I histocompatibility molecules [58], viral proteins [157] or epidermal growth factor receptor [117]. However, the mobility of class II major histocompatibility antigen was substantially increased after removal of cytoplasmic domains [180]. The apparent discrepancies between aforementioned results can be resolved if it is suggested that the mobility of membrane molecules is limited by i) extensive interactions between the extracellular domains of most molecules and ii) interactions between the intracytoplasmic domains of some molecular species and cytoskeletal elements. This concept is supported by recent experimental data. The diffusion constant of class I major histocompatibility molecules ( $L^d$ ) that were either native or deprived of 1, 2 or 3 glycosylation sites was determined [185]:  $D$  increased from  $6 \times 10^{-10}$  to  $17 \times 10^{-10} \text{ cm}^2/\text{s}$ . In other experiments, chimeric molecules with transmembrane or glycosylphosphatidylinositol linkage and extracellular domains from Thy-1 molecule, placental alkaline phosphatase or vesicular stomatitis virus G proteins were studied. It was concluded that ectodomains accounted for the major part of resistance to displacement [190]. Further, lymphocytes were transfected with genes coding for wild-type CD8 molecules or CD8 molecules with extensive deletion of intracellular and transmembrane domains. They were exposed to anti-CD8 antibodies in order to induce capping [174]: similar redistribution of cytoskeletal elements was found, suggesting that interactions between CD8 molecules and microfilaments were mostly mediated by interactions between extracellular domains of membrane molecules [9]. Finally, a recent study made on the movements of cell surface histocompatibility molecules labeled with colloidal gold [58] revealed that the long-distance displacements were limited by a dynamic (temperature dependent) barrier, restricting the amplitude of most movements to less than  $1 \mu\text{m}$ . In conclusion, cell surface glycoproteins comprise a substantial fraction of immobile elements (diffusion constant less

than  $10^{-12}$  cm<sup>2</sup>/s) and a fraction of similar importance with a diffusion constant ranging between  $10^{-10}$  and about  $3 \times 10^{-9}$  cm<sup>2</sup>/s. Movements are essentially restrained by extensive interactions between extracellular domains of membrane molecules and occasional interaction between some intracellular domains and cytoskeletal elements. Finally, it must be recalled that cross-linking membrane molecules may result in enhancing their interactions with microfilaments [74] and large scale redistribution (as exemplified by the capping phenomenon [174]).

*Conclusion.* We have now reviewed some biophysical properties of living cells, with

Fig. 12. Solid-like behavior of a cell. Human melanoma cells were sucked into micropipettes [8]. The tip of protrusions (arrows) is not spherical, indicating that the cell did not behave as a liquid. Bar is  $8 \mu\text{m}$ .

a particular emphasis on leucocytes. The quantitative estimates of different cell parameters will be used to discuss the relevance of different theoretical models to the adhesive behavior of these cells. A tentative sketch of the cell surface is shown on fig. 11.

#### 4. Models for the sequential steps of cell adhesion

We shall now discuss the relevance of different theoretical models to the adhesion of nucleated cells. As emphasized in the first section of this review, our point is not to describe basic concepts and results obtained by physicists and physical chemists, but to make use of available data to select the theories that seem most relevant to cell biology. We shall consider sequentially the following steps of the adhesive process:

- Cell-cell or cell-substrate approach.
- Initial bond formation.
- Cell membrane reorganization in contact areas.
- Cell-substrate detachment.

##### 4.1. Cell-cell approach

The probability of bond formation between two cells or a cell and a solid surface bearing complementary molecules is obviously dependent on the mutual force exerted by approaching structures. The complexity of cell membranes would make hopeless any rigorous attempt at achieving an *ab initio* derivation of these forces. Indeed, we may quote the introductory sentence of the celebrated book by Eyring and colleagues [73] “In so far as quantum mechanics is correct, chemical questions are problems in applied mathematics. In spite of this, chemistry, because of its complexity, will not cease to be in large measure an experimental science ...”.

The complexity of cellular and colloidal systems led many authors to focus on particular noncovalent interactions that may not be independent. Thus, in a recent paper [176], Van Oss reviewed 17 interactions that might be reduced to a lesser number of more ‘fundamental’ forces. We shall only mention a few approaches to cell interactions.

##### 4.1.1. Conditions of contact formation

In order to estimate quantitatively the relevance of a given interaction to cell adhesion, we need some guidelines for performing rough calculations. In view of aforementioned data, the initial contact should involve the tip of microvilli. This is indeed supported by morphological studies made on the initial step of platelet aggregation [79], mutual adhesion of embryonic neural retina cells [17] or concanavalin A-induced fibroblast agglutination [186]. The initial contact area should thus be in the order of  $0.01 \mu\text{m}^2$  (or  $10^{-14} \text{m}^2$ ).

The minimal binding energy required to influence cell adhesion is in the order of  $kT$  (where  $k$  is Boltzmann’s constant and  $T$  is the absolute temperature), since bond formation cannot occur if cells are not maintained against thermal agitation. The corresponding value is about  $4 \times 10^{-21} \text{J}$ .

Further, a repulsive force cannot influence adhesion if it is weaker than the sedimentation force (during *in vitro* experiments), i.e. about  $10^{-13}$  N. Also, it is likely that under *in vivo* conditions where cells are often bound to matrix components, the minimal force required to influence the formation of new adhesions is the protrusive force of cell microvilli. Although this is not well known, a reasonable order of magnitude is about  $10^{-11}$  N, corresponding to the force required in order that a cylindrical microvillus of  $0.1 \mu\text{m}$  diameter progress against the basal tension of a resting neutrophil [72]. This force is similar to the sedimentation force under mild centrifugation.

Finally, it must be noted that a reasonable value for the interbilayer distance during the association of membrane intrinsic receptors is twice the size of extracellular domains, i.e. between 10 and 20 nanometers.

The above estimates will be used to test the relevance of several interactions to cell adhesion.

The experimental success met by the DLVO theory of the stability of lyophobic colloids (independently elaborated by Derjaguin and Landau, and Verwey and Overbeek) prompted its application to biological systems [39]. The basic idea was to consider the balance between Van der Waals attraction and electrostatic repulsion (see, e.g., [24] for a review with reference to biological cells).

#### 4.1.2. Electrodynamic attraction

The unretarded force  $F$  between two parallel lipid bilayers with thickness  $a$  and distance  $d$  is attractive, with intensity (per unit area)

$$F = (A/6\pi)(1/d^3 - 2/(d+a)^3 + 1/(d+2a)^3) \quad (11)$$

where  $A$  is called the Hamaker constant. Its value is of the order of  $5 \times 10^{-21}$  J in aqueous medium [98]. The corresponding energy  $W$  is given by

$$W = -(A/12\pi)(1/d^2 + 1/(d+2a)^2 - 2/(d+a)^2). \quad (12)$$

Considering two lipid bilayers of width  $0.45 \text{ nm}$  and area  $0.01 \mu\text{m}^2$  separated by a gap of  $10 \text{ nm}$  width, the attractive force and energy are respectively  $1.3 \text{ piconewton}$  and  $1.1 kT$  respectively (table 3). These values are negligible under standard experimental conditions.

#### 4.1.3. Electrostatic repulsion

Since cells bear a net negative charge, they are expected to exert a mutual repulsion. In biological media, this repulsion is much lower than it would be in vacuum, since it is screened by water (with a relative dielectric constant of about 80) and electrolytes. In dilute solutions, it may be shown that the presence of free ions results in dividing the interaction potential between two charges at distance  $r$  by a factor of  $\exp(Kr)$ , where  $1/K$  is the 'Debye-Hückel length' (see, e.g., [24] for a brief review). This parameter can be calculated with the formula

$$K = \left( \sum_i c_i q_i^2 / \epsilon kT \right)^{1/2} \quad (13)$$

where the summation is over all ion species of concentration  $c_i$  (molecules/m<sup>3</sup>) and electric charge  $q_i$ ,  $k$  is Boltzmann's constant,  $\varepsilon$  is the dielectric constant of water and  $T$  is the absolute temperature. In 150 mM NaCl solutions, the limit of validity of the simple theory is reached, but this can be used when electric fields are low. The Debye–Hückel length is about 0.8 nm and the interaction force and energy per unit area between two parallel plates with surface charge and separation  $d$  is [24, 98]

$$F \approx (2\sigma^2/\varepsilon) \exp(-Kd), \quad (14)$$

$$W \approx 2(\sigma^2/\varepsilon K) \exp(-Kd). \quad (15)$$

Considering two plates with surface charge equal to 0.02 C/m<sup>2</sup> and distance 10 nm, and 0.01  $\mu\text{m}^2$  area,  $F$  and  $W$  are respectively  $4.2 \times 10^{-14}$  N and 0.008  $kT$ . These values are too low to influence bond formation.

However, the above calculation is based on the unwarranted assumption that the negative electric charge of cell membranes is concentrated near the phospholipid bilayer. If this charge is considered as scattered over the whole glycocalyx, another treatment is required. The simplest procedure is to consider these charges as uniformly distributed in a layer of thickness  $L$ . Since the charge density is low, we may use the simplest form of Debye–Hückel theory, and write the interaction energy between two charges  $q$  and  $q'$  separated by a distance  $r$  as

$$W = (qq'/4\pi\varepsilon r) \exp(-Kr). \quad (16)$$

The electrostatic energy of the cell coat is then readily calculated as

$$W = \sigma^2/2\varepsilon K^2 L \quad (17)$$

where  $\sigma$  is the equivalent surface charge density (i.e. volume density multiplied by cell coat thickness  $L$ ). If we assume that cell coats are uniformly compressed when

Table 3  
Order of magnitude of several intercellular forces (for a contact area of  $10^{-14}$  m<sup>2</sup> and interbilayer distance of 10 nm).

Interaction	Force (piconewton)	Energy (kT units)
Electrostatic:		
– charges on lipid polar groups	0.04	0.008
Electrostatic:		
– uniform volume distribution	72	125
Van der Waals attraction	1	1
Compression of surface anchored chains	9	50
Single molecular bond	5	10–20

The magnitude of several interactions was evaluated as described. It is concluded that cell-bound polyelectrolytes may prevent bond formation in usual conditions of encounter.

the cell surfaces are separated by a distance  $d$  lower than  $L$ , the interaction energy may be readily calculated as

$$W = \sigma^2(4/d - 2/L)/2\epsilon K^2. \quad (18)$$

Taking  $L$  as 20 nm and  $d$  as 10 nm, we obtain the estimates

$$F = 30 \text{ nanonewton}, \quad W = 124 kT$$

for the repulsive force  $F$  and the energy  $W$  for an interaction area of  $10^{-14} \text{ m}^2$ . These values are not negligible. However, we used very crude assumptions and more refined estimates might be needed. As will be discussed now, the most satisfactory approach from a theoretical point of view might be to use the framework of polymer theory and consider cell surfaces as coated with bound polyelectrolyte layers.

#### 4.1.4. Cell-cell repulsion as an example of steric stabilization

The need to prepare stable colloid dispersions is often encountered in industrial practice. Indeed, micrometer size hydrophobic particles will spontaneously agglutinate in aqueous media unless some repulsive interaction prevents mutual approach. Hence, it may be argued that the problem of living cells may be to prevent useless adhesion as well as initiating purposeful contacts.

Electrostatic stabilization is achieved by coating colloid particles with charged groups. However, this is known to be inefficient in ionic solutions such as biological media [137] due to the screening of repulsive forces by counterions. Under these conditions, agglutination may be prevented by coating particles with adsorbed or grafted macromolecules. This is (unfortunately?) called steric stabilization. Much experimental and theoretical work was done to clarify this phenomenon. We refer the reader to recent reviews for more information on polymer physics [46], polymer at interfaces [47, 48] and especially steric stabilization [137]. We give only a brief summary of the problems encountered when applying these concepts to cellular systems.

The basic framework for describing long flexible chains is described in Flory's book [75]. A chain may be visualized as a sequence of  $N$  linear segments of length  $l$  with free rotation at the intersections. If rotation is hindered by molecular interactions, it is possible to consider an 'equivalent' chain with  $N'$  segments of length  $l'$  with free rotation ( $N' < N$  and  $l' > l$ ). The chain static conformation may be viewed as a weighted average of a large set of conformations. The probability  $P(c)$  of each conformation  $c$  is given by

$$P(c) = \exp(-F(c)/kT)/Z \quad (19)$$

where the partition function  $Z$  is given by

$$Z = \sum_{\{c\}} \exp(-F(c)/kT) \quad (20)$$

where  $k$  is Boltzmann's constant,  $T$  is the absolute temperature and  $F(c)$  is the free energy contribution of segment-segment, segment-solvent and solvent-solvent interactions. The partition function  $Z$  is related to the total free energy  $F$  by the standard formula

$$F = -kT \ln(Z). \quad (21)$$

Note that dynamic aspects are not considered.

If solvent and monomer groups are similar, all  $F(c)$  are identical. This situation usually occurs at a well defined temperature (since  $F(c)$  is usually dependent on  $T$ ) which is called the  $\theta$  temperature. One may also refer to a  $\theta$  solvent. All configurations are then equivalent, which makes easier the determination of  $Z$  with statistical techniques (see [5] for a compact presentation as a prerequisite to dynamical studies). The 'root mean square end-to-end distance' (i.e. the square root of the mean square of end-to-end distance) is thus simply  $l\sqrt{N}$ . Another quantity of interest is the radius of gyration ( $R_g$ ), that is defined as usual as the square root of the mean squared distance between the center of gravity of the chain and monomers.

$$R_g = l\sqrt{(N/6)}. \quad (22)$$

Now, the number of possible configurations is reduced by the constraint that only one monomer can be located at a given point. The partition function is further reduced in non- $\theta$  conditions. As indicated in section 3, water is a good solvent for polysaccharides found on the cell surface. This means that monomer-monomer interactions result in a free energy increase. This leads to a reduction of the probability of occurrence of more compact configurations, and the radius of gyration varies as  $N^{0.6}$  rather than  $\sqrt{N}$ .

Consider now cell-to-cell approach. This may result in a free energy increase for several different reasons:

- i) When the intercellular distance is less than twice the extended length of surface chains, there is a reduction of possible configurations and increased weight of monomer-monomer interactions. In a good solvent, this results in a free energy increase that may be viewed as a mixing free energy.
- ii) If the extended length ( $Nl$ ) of chains is higher than the interbilayer distance, some configurations are made impossible, and compact configurations, with monomer-monomer interactions, are favored. This interaction may be viewed as a chain compression effect.
- iii) The interaction is made more complex if intermolecular associations (specific or non specific, see below) occur between cell surfaces. In this case, bridges may be formed between surfaces and negative free energy variations can be observed. Also, if surface chains are adsorbed rather than anchored, desorption or adsorption phenomena can occur. It is very difficult to account for these phenomena, however, we shall neglect them in the present section. This simplification may be valid if intermolecular associations are treated separately, and if cell-cell approach is too rapid to allow adsorption or desorption.

As emphasized by Israelachvili in his recent monograph [98], there is no universal 'ready-to-use' theory of steric stabilization. Also, the presence of charged groups on cell surface polymers makes more difficult the application of many current models. Therefore, in view of available results, we propose the following approach, while emphasizing that more work is clearly needed in this domain:

First, it was noted that several hours were required for equilibrium during the mutual approach between mica surfaces bearing polymer molecules in a good solvent [100]. Hence, it seems warranted to neglect polymer adsorption and desorption during the first steps of cell-to-cell approach and refer to interactions between surfaces with grafted, non-adsorbing polymers.

Secondly, if we model cell surface polymers as linear molecules with 1,000 units of monomers each and an mean of 0.5 monomer per  $\text{nm}^2$ , the mean distance between chains is in the order of  $1/\sqrt{(0.0005)} = 45$  nm. This is not very different from the glycocalyx thickness, which suggests that chains may be considered as fairly independent (this is the so-called 'mushroom regime' defined by de Gennes).

If we neglect chain-chain interaction, we may estimate the compression contribution to cell-cell repulsion by making use of a theory elaborated by Dolan and Edwards who first treated the  $\theta$ -solvent case [54] and later extended their calculation to a more general situation allowing monomer-monomer repulsion and excluded volume effects. The latter theory was much more complex and did not yield simple analytical formulae [55]. Since we are mainly interested in order-of-magnitude estimates, we shall use the results obtained in the first paper. The authors obtained two different formulae with complementary ranges of validity. For large separations  $d$  of the plane surfaces (greater than  $l\sqrt{N}$ ), the free energy was found to be

$$F = -kT \ln (1 - 2 \exp(-3d^2/2Nl^2)). \quad (23)$$

For small separations ( $d$  smaller than about  $1.7l\sqrt{N}$ ), they obtained

$$F = -kT \left( \ln (d\sqrt{(3/8\pi N)/l}) - \pi^2 l^2 N/6d^2 \right). \quad (24)$$

This result was very conveniently simplified by Israelachvili [98]. When the distance between the cell surfaces ranges between  $2R_g$  and  $8R_g$ , where  $R_g$  is the radius of gyration, the repulsive free energy per chain is

$$W \approx 36kT \exp(-d/R_g). \quad (25)$$

Assuming a monomer density  $\Gamma$  of 0.5 monomer per  $\text{nm}^2$  and a mean number of 1,000 monomers per chain, the interaction between two cells separated by a gap of 10 nm with a contact area of  $0.01 \mu\text{m}^2$  is

$$F = 180kT \exp(-10/R_g) \quad (26)$$

where  $R_g$  is expressed in nanometer. A minimal estimate of  $R_g$  for standard cells would be about 8 nm, assuming a value of 0.6 nm for  $l$  (this is the length of an

hexasaccharide group [102] and using equation (22). The minimal value of  $W$  would then be about  $50kT$  with a corresponding force of  $50kT/R_g \approx 8.8 \times 10^{-12}$  newton. It is concluded that steric stabilization may significantly impair the contact between cell microvilli. It is thus warranted to look for more precise data on these interactions. In this respect, it is worth recalling that the occurrence of fairly long-ranged repulsion between surfaces bearing adsorbed electrolytes was demonstrated experimentally with Israelachvili's surface force apparatus [118].

#### 4.1.5. Other interactions

We refer the reader to specialized reviews for more details on diverse interactions that are not obviously relevant to nucleated cells [98]. We only mention some of these forces.

When the distance between two molecularly smooth surfaces is of the order of several diameters of solvent molecules (i.e. 0.2 nm for water), very strong forces may be generated by the ordering of these molecules in sequential planes parallel to the surfaces. Repulsive [116], attractive [99] or even oscillatory [98] forces were thus described. The intensity exhibits a fairly exponential decay with a characteristic length in the order of several tenths of nanometer. These interactions are not likely to play a role in cell-cell adhesion, since the interbilayer distance remains fairly high, and interacting surface are not molecularly smooth. However, these interactions might play a role in membrane fusion.

When the distance between two flexible surfaces is decreased, the shape fluctuations due to thermal agitation may be somewhat inhibited, which results in a repulsive force [92]. This interaction may be significant when very flexible structures such as lipid vesicles or erythrocytes are considered [70]. However, this must be much weaker when nucleated cells are considered, since their membranes are much more rigid.

Finally, the exclusion of macromolecules in the intercellular space may result in osmotic attraction. The force per unit area is simply  $nkT$ , where  $n$  is the macromolecule concentration in the bulk medium. The adhesive energy per unit area is  $nkTD$ , where  $D$  is the diameter of macromolecules. Considering plasma as a representative medium, the major macromolecule is albumin with a concentration in the order of  $3.9 \times 10^{23}$  molecules/m<sup>3</sup> and a diameter in the order of 5 nm. The corresponding force and energy for an interaction area of  $0.01 \mu\text{m}^2$  are respectively  $1.6 \times 10^{-11}$  newton and  $20kT$ . However, the exclusion of these molecules from contact area may depend on the tightness of adhesion [135]. Indeed, the possibility of performing immunofluorescence labeling in regions of contact between cytotoxic T lymphocytes and target cells suggests that molecules as large as immunoglobulin G (MW 150,000) are not always excluded from adhesion areas [6].

## 4.2. Initiation of adhesion

### 4.2.1. Surface energy approach

We shall only add some comments to the experimental results described in section 2.3.1.

A thermodynamic approach would seem in principle ideally suited to obtain general results concerning complex systems. Thus, it seems reasonable to try and derive the work of adhesion between cell surfaces from parameters measured on isolated cells. The aforementioned finding that equilibrium may not be reached before a very prolonged contact does not suffice to invalidate this approach, since many empirical procedures may be used to deal with systems that were in fact out of equilibrium (see for example discussions concerning contact angle hysteresis [4]).

The simplest approximation, first discovered by Raleigh and further emphasized by Good and colleagues [84] was to express the work of adhesion between two substances (1) and (2) as

$$W_{12} = p_1 p_2 \quad (27)$$

where  $p_1$  and  $p_2$  are intrinsic parameters of media (1) and (2). This formula yields

$$\gamma_{12} = \gamma_1 + \gamma_2 - 2\sqrt{\gamma_1 \gamma_2} \quad (28)$$

connecting the interfacial free energy  $\gamma_{12}$  of the (1–2) interface to the surface energies  $\gamma_1$  and  $\gamma_2$  of (1) and (2). It was soon recognized that this relationship only held between limited series of liquid media and it was suggested to split surface energies into several components. The most popular procedure was to discriminate between London ('dispersion') and polar components (see, e.g., [104]) and write

$$\gamma = \gamma^d + \gamma^p. \quad (29)$$

Thus, the surface free energy of water (73 mJ/m<sup>2</sup>) was written as a sum of a minor dispersive component (21 mJ/m<sup>2</sup>) and a major polar component (52 mJ/m<sup>2</sup>). Equation (23) is then replaced with

$$\gamma_{12} = \gamma_1 + \gamma_2 - 2\sqrt{\gamma_1^d \gamma_2^d} - 2\sqrt{\gamma_1^p \gamma_2^p}. \quad (30)$$

Other more sophisticated formulae were used (e.g., harmonic mean instead of geometric mean) without marked conceptual difference. A significant progress was the introduction of the concept of monopolar surfaces by Van Oss and colleagues [117], who emphasized the difference between molecules with a dipolar moment, and molecules with the capacity to form hydrogen bonds, either as proton donors or acceptors. They suggested that numerous biopolymers were in fact 'monopolar', by acting essentially either as electron donors or electron acceptors. Thus, they wrote the surface energy of a medium as

$$\gamma = \gamma^{LW} + \gamma^+ + \gamma^- \quad (31)$$

thus defining a Lifshitz–Van der Waals term, a proton-donating and a proton-accepting term. Finally, they suggested that the three interfacial components of a surface might be determined experimentally by contact angle determinations, using as test liquids diodomethane (an essentially apolar substance), dimethylsulfoxide (a liquid with an

essentially zero proton-donating component) and, e.g., water, where  $\gamma^+$  and  $\gamma^-$  were set equal for the sake of convenience.

However, several problems make difficult the application of the aforementioned concepts to biological systems.

Firstly, the combination rules we mentioned can be subjected to direct experimental check only if all tested phases are liquid, thus allowing straightforward determination of all interfacial energies. However, the study of the surface properties of solids is much more difficult to achieve. This is a major difficulty, since the behavior of solid surfaces may be quite different from that of liquids [5] and cell surfaces cannot be treated as liquid structures. The impossibility to perform a direct test of theoretical formulae makes it difficult to assess the value of new ideas.

Secondly, even the incomplete measurements that can be performed on solid surfaces raise specific problem. Thus, the contact angles measured on cell monolayers depend on the conditions of preparation of these monolayers, which supports the suggestion that we are not dealing with equilibrium parameters [130]. Several authors studied the surface properties of biological cells by studying their partition between two immiscible phases [156]. This approach is quite attractive, but the derivation of quantitative parameters from experimental data is not straightforward.

Thirdly, whereas usual surface energies are in the order of several tens of  $\text{mJ/m}^2$ , the intercellular interaction energies are much lower (see section 2). This means that there is a need for very accurate combination rules. These are not available at the present time.

Fourthly, it must be reminded that 'specific' interactions are not accounted for by the thermodynamic approach. This may be a problem with biological systems since many low-affinity interaction between complementary structural groups are probably involved in cell-cell interactions (e.g., interactions involving RGDS sequences described in section 2).

In conclusion, whereas the thermodynamic approach met with some success in describing the interaction between cells and polymer surfaces (see in this respect an interesting attempt as relating the thermodynamic approach to DLVO theory [179]), more work is needed before it may be used to assess the importance of nonspecific interactions between cells bound by specific ligands.

#### 4.2.2. Consideration of ligand-receptor bonds

A fairly simple and powerful theoretical framework was suggested by George Bell [15] who emphasized several important ideas.

First, he obtained estimates for the kinetics of bond formation between membrane-associated molecules. The basic idea was to use the forward and reverse kinetic constants  $k_f$  and  $k_r$  for the equilibrium



The ratio  $k_f/k_r$  represents the equilibrium constant  $K$ , which was considered as independent of diffusion constants: this assumption allowed to use for  $K$  the range of values measured for association between soluble molecules. The approximation

was to neglect the difference between soluble and membrane molecules with respect to the free energy increase due to the loss of degrees of freedom as a consequence of complex formation. It was thus possible to estimate a reasonable order of magnitude for the maximum rate of bond formation as

$$dN_b/dt < 1.3 \times 10^{-2} N_1 N_2 \mu\text{m}^{-2} \quad (33)$$

where  $N_b$ ,  $N_1$  and  $N_2$  are the numbers of complexes (1–2) and free molecules (1 or 2) on interacting cells per squared micrometer.

An other important point was the estimate of the maximum strength of a molecular bond: Bell estimated at about  $10^{-11}$  newton the force required to uproot a receptor. This value was very close to experimental estimates later obtained by Goldsmith [169] and Evans [66].

Another concept emphasized by Bell [15] was an estimate of the effect of tension on the lifetime of a molecular bond. Using experimental data obtained on the lifetime of material samples subjected to varying loads [192], Bell suggested the following formula for the rate of bond dissociation:

$$k_r = k_{r0} \exp(\Gamma F/kTN_b) \quad (34)$$

where  $F$  is the total disruptive force,  $N_b$  is the number of bonds (the force is thus  $F/N_b$  per bond) and  $\Gamma$  is a constant that was taken as 0.5 nm.

The framework suggested by Bell was extended by Hammer and Lauffenburger [88] who considered the dynamic adhesion of cells to adhesive substrates in a viscous shear flow. They took care of the mobility of cell surface receptors and stress applied to molecular bonds. They were thus able to define a rate-controlled high affinity regime and a affinity-controlled low-affinity regime. In a later paper, this model was extended to a probabilistic framework accounting for the fluctuations of bond number [38]. This point was of obvious importance since adhesion can be initiated by very few bonds, and initial attachment is heavily dependent on the duration of the first bond. The authors concluded that the previous deterministic approach could underestimate the time needed for cell attachment and overestimate the time required for cell detachment.

The aforementioned approach was extended along different lines by Dembo and colleagues [49] who coupled the equations for deformation of an elastic membrane with equations for the kinetics of bond formation. They introduced the concept of ‘catch bond’ by noticing that the disruption of a stretched bond might be in principle slower than that of an unstressed bond. This is consistent with thermodynamic principles if the formation of stressed bonds is also much slower than the formation of unstressed ones. This concept is important since it suggests the interest of studying the effect of stress on the kinetic constants of bond formation and dissociation. This may be useful to understand the significance of different ligand-receptor couples recently demonstrated on the membranes of different cell populations. This may also be important to understand the conditions required for ‘rolling’ as described in section 2. However, more experimental data are required to support the validity of this interesting concept.

### 4.3. Analysis of the 'equilibrium' shape of cell-cell contacts

Electron microscopical studies of cell-cell contact areas demonstrated that the extension of the adhesive area [31] or the tightness of apposition between bound membranes [29] were increased when the adhesive bond density was increased [31] or nonspecific repulsive forces were decreased [29, 129]. It was thus tempting to build a model for the equilibrium shape of intercellular contact. Bell and colleagues [16] described a model of cell-cell adhesion with a balance between bond formation by mobile ligand and receptor molecules and nonspecific repulsion. Using phenomenological expressions for the repulsive force and bond elasticity, they estimated the equilibrium contact area and intermembrane distance with complete neglect of the cell mechanical behavior. Hence, this approach yielded a thermodynamic limit for the contact area. They stressed that active movements of one or another of the cells could however influence the kinetics of contact formation.

Other models of adhesion between solid surfaces described binding as a balance between adhesive surface forces and mechanical resistance of the surfaces. A basic model was described by Johnson and colleagues [101] to account for the adhesion of two solid elastic spheres with contact forces. They cleverly adapted Hertz's theory for the contact deformation of two spheres pushed against each other by a known load  $P$ . The main results of the adhesion theory may be sketched as follows. The radius  $a$  of the contact disc between a sphere of radius  $R$  and a rigid plane is

$$a = (R/K)(P + 3\Gamma R + \sqrt{-6\Gamma\pi RP + 9\Gamma^2\pi^2 R^2}) \quad (35)$$

where  $\Gamma$  is the work of adhesion per unit area and  $K$  is given by

$$K = (1 - \sigma^2)/(\pi E) \quad (36)$$

where  $\sigma$  is Poisson ratio and  $E$  is Young modulus. Another result is that the force required to separate surfaces is

$$P = -3\Gamma\pi R/2. \quad (37)$$

A difficulty with this theory is that infinite stress was predicted at the rim of the contact disc. This led Derjaguin and colleagues to introduce noncontact forces [51] (in fact, the first author of the latter paper had studied the effect of contact deformation on adhesion as soon as 1934, see [51]). These theories proved a sound basis to study the adhesion of solids, and they were subjected to experimental check [95]. Also, they were used to account for the interaction between rough surfaces by modeling asperities as protrusions with spherical tip and varying length [85]. These theories prompted later attempts at accounting for the modification of cell surface roughness in regions of contact with smooth surfaces. Rat macrophages were made to bind smoother glutaraldehyde-treated erythrocytes, and electron micrographs were used to measure the roughness of the macrophage membrane in free and contact areas. Then, assuming that the major part of the macrophage resistance to smoothing was located in microvilli, the adhesive energy was derived by considering the balance

between macrophage mechanical properties and adhesive forces [129]. However, the validity of the basic assumption was, admittedly, very difficult to check thoroughly.

A more rigorous approach was undertaken by Evans who derived the work of adhesion between the smooth surfaces of lipid vesicles or erythrocytes by measuring the encapsulation of a more rigid vesicles by a flaccid one, and considering the equilibrium between adhesive energy and mechanical resistance of interacting surfaces [69]. Also, he provided theoretical models of membrane-membrane adhesion where he incorporated the effects of membrane resistance to bending and tension as well as bond stretching. In the case of a continuum of molecular cross-bridges, the classical Young equation was found to be consistent with the model [64]. When he used a discrete distribution of cross-bridges, two interesting conclusions were reached [65]. First, the minimum tension required to separate adherent membranes might be different from the maximum tension induced in the membrane during contact formation. Secondly, he demonstrated the existence of lateral forces exerted on bonding structures, which might result in bond accumulation in contact zones during cell-cell separation. This possibility was strongly supported by the finding that increased membrane tension increased during the separation of lectin-attached red cells [68] as well as conjugated cytotoxic lymphocytes and target cells [172]. The latter experimental study prompted the elaboration of a dynamic model of conjugate formation involving a lateral diffusion of membrane molecules [171].

In conclusion, it seems now well established that the structure of cell-cell contact area is dependent on several well defined parameters such as bond energy, lateral mobility of binding molecules, bond elasticity, mechanical resistance of the cell membrane, nonspecific repulsion between interacting cells. Many models were elaborated to integrate these parameters into an unified theoretical framework. The main difficulty is that specific approximations are required to make these models tractable. This is possible only if the experimental values of numerical parameters or the behavior of empirical force/distance curves are known. However, these parameters are not known with sufficient accuracy at the present time. Also, it is likely that different biological systems behave in quite different ways, and a single workable model may not account for all situations of physiological interest. However, much progress was done during the last years and a reliable modeling of cell-cell initial adhesion no longer seems an impossible goal.

#### 4.4. Cell-cell separation

Many aforementioned reports demonstrated that cell adhesion does not behave as a reversible process. Indeed, initial contact is rapidly followed by several active processes such as reorganization of membrane molecules, cytoskeletal concentration in adhesive regions, and possibly glycocalyx reorganization in order to minimize repulsion. It is therefore not surprising that the minimal force required to prevent bond formation may be much lower than the force required to detach bound cells (see, e.g., [128]). Indeed, cell separation may often be considered either as an active process where the cell chooses to release its 'grip' [146]. Alternatively, forced cell detachment may reflect membrane rupture rather than bond dissociation (see, e.g., [26]). Hence, the process of cell separation will not be further discussed in the present review.

## Conclusion

The aim of this work was to describe present experimental and theoretical knowledge on the initial steps of cell adhesion. Since this encompasses many different fields of physics and biology, we chose to present a brief and incomplete sketch of available data, in order to make important issues more apparent. Our hope is that this will help biophysicists to enter the fascinating field of cell adhesion.

## References

1. Abbas, A.K., K.A. Ault, M.J. Karnovsky and E.R. Unanue, 1975, Non random distribution of surface immunoglobulin on murine B lymphocytes, *J. Immunol.* **114**, 1197–1204.
2. Absolom, D.R., C.J. van Oss, W. Zingg and A.W. Neumann, 1982, Phagocytosis as a surface phenomenon. Opsonization by aspecific adsorption of IgG as a function of bacterial hydrophobicity, *J. Reticuloendothelial Soc.* **31**, 59–70.
3. Absolom, D.R., W. Zingg, C. Thomson, Z. Policova, C.J. van Oss and A.W. Neumann, 1985, Erythrocyte adhesion to polymer surfaces, *J. Colloid Interface Sci.* **104**, 51–59.
4. Adamson, A.W., 1982, *Physical Chemistry of Surfaces* (Wiley, New York).
5. Andrade, J.D., S.M. Ma, R.N. King and D.E. Gregonis, 1979, Contact angles at the solid-water interface, *J. Colloid Interface Sci.* **72**, 488–494.
6. André, P., A.M. Benoliel, C. Capo, C. Foa, M. Buferne, C. Boyer, A.M. Schmitt-Verhulst and P. Bongrand, 1990, Use of conjugates made between a cytolytic T cell clone and target cells to study the redistribution of membrane molecules in cell contact areas, *J. Cell Sci.* **97**, 335–347.
7. André, P. and P. Bongrand, 1990, Cell-cell contacts, in: *Biophysics of the Cell Surface*, eds R. Glaser and D. Gingell (Springer, Berlin) pp. 287–322.
8. André, P., C. Capo, A.M. Benoliel, P. Bongrand, F. Rougé and C. Aubert, 1990, Splitting cell adhesiveness into independent measurable parameters by comparing ten human melanoma cell lines, *Cell Biophys.* **17**, 163–180.
9. André, P., J. Gabert, A.M. Benoliel, C. Capo, C. Boyer, A.M. Schmitt-Verhulst, B. Malissen and P. Bongrand, 1991, Wild type and tailless CD8 display similar interaction with microfilaments during capping, *J. Cell Sci.* **100**, 329–337.
10. Arnott, S., A. Rees and E.R. Morris, 1983, *Molecular Biophysics of the Extracellular Matrix* (Humana Press, Clifton).
11. Atherton, A. and G.V.R. Born, 1972, Quantitative investigations on the adhesiveness of circulating polymorphonuclear leukocytes to blood vessel walls, *J. Physiol.* **222**, 447–474.
12. Ault, K.A. and E.R. Unanue, 1978, in: *Theoretical Immunology*, eds G.I. Bell, A.S. Perelson and G.H. Pimbley (Marcel Dekker, New York) pp. 145–169.
13. Baier, R.E. and L. Weiss, 1975, Demonstration of the involvement of adsorbed proteins in cell adhesion and cell growth on solid surfaces, *Adv. Chem. Ser.* **145**, 300–307.
14. Baumgartner, H.R., T.B. Tschopp and D. Meyer, 1980, Shear rate dependent inhibition of platelet adhesion and aggregation on collagenous surfaces by antibodies to human factor VIII/von Willebrand factor, *Br. J. Haematol.* **44**, 127–139.
15. Bell, G.I., 1978, Models for the specific adhesion of cells to cells, *Science* **200**, 618–627.
16. Bell, G.I., M. Dembo and P. Bongrand, 1984, Cell adhesion – competition between nonspecific repulsion and specific bonding, *Biophys. J.* **45**, 1051–1064.
17. Ben Shaul, Y. and A. Moscona, 1975, Scanning electron microscopy of aggregating embryonic neural retina cells, *Exp. Cell Res.* **95**, 191–204.
18. Berke, G., 1980, Interaction of cytotoxic T lymphocytes and target cells, *Prog. Allergy* **27**, 69–133.
19. Bevilacqua, M.P., S. Stengelin, M.A. Gimbrone and B. Seed, 1989, Endothelial leukocyte adhesion molecule 1: An inducible receptor for neutrophils related to complement regulatory proteins and lectins, *Science* **243**, 1160–1165.
20. Bierer, B.E., B.P. Sleckman, S.E. Ratnovsky and S.J. Burakoff, 1989, The biologic roles of CD2, CD4 and CD8 in T cell activation, *Annu. Rev. Immunol.* **7**, 579–599.

21. Bjorkman, P., M. Saper, B. Samraoui, W. Bennett, J. Strominger and D. Wiley, 1987, Structure of the human class I histocompatibility antigen HLA-A2, *Nature* **329**, 506–512.
22. Bongrand, P., 1988, *Physical Basis of Cell-Cell Adhesion* (CRC Press, Boca Raton, FL).
23. Bongrand, P. and G.I. Bell, 1984, Cell-cell adhesion: Parameters and possible mechanisms, in: *Cell Surface Dynamics: Concepts and Models*, eds A.S. Perelson, C. DeLisi and F.W. Wiegel (Marcel Dekker, New York) pp. 459–493.
24. Bongrand, P., C. Capo and R. Depieds, 1982, Physics of cell adhesion, *Prog. Surf. Sci.* **12**, 217–286.
25. Bongrand, P., C. Capo, J.L. Mège and A.M. Benoliel, 1988, Use of hydrodynamic flows to study cell adhesion, in: *Physical Basis of Cell-Cell Adhesion*, ed. P. Bongrand (CRC Press, Boca Raton, FL) pp. 125–156.
26. Bongrand, P. and P. Golstein, 1983, Reproducible dissociation of cellular aggregates with a wide range of calibrated shear forces: Application to cytolytic lymphocyte-target cell conjugates, *J. Immunol. Methods* **58**, 209–224.
27. Bongrand, P., M. Pierres and P. Golstein, 1983, T cell-mediated cytotoxicity: On the strength of effector-target cell interaction, *Eur. J. Immunol.* **13**, 424–429.
28. Buxbaum, R., E. Evans and D.E. Brook, 1982, Quantitation of surface affinities of red blood cells in dextran solutions and plasma, *Biochemistry* **21**, 3235–3239.
29. Capo, C., P. Bongrand, A.M. Benoliel, A. Ryter and R. Depieds, 1981, Particle-macrophage interaction: Role of surface charges, *Ann. Immunol. (Inst. Pasteur)* **132D**, 165–173.
30. Capo, C., F. Garrouste, A.M. Benoliel, P. Bongrand and R. Depieds, 1981, Nonspecific binding by macrophages: Evaluation of the influence of medium-range electrostatic repulsion and short-range hydrophobic interaction, *Immunol. Commun.* **10**, 35–43.
31. Capo, C., F. Garrouste, A.M. Benoliel, P. Bongrand, A. Ryter and G.I. Bell, 1982, Concanavalin A-mediated thymocyte agglutination: A model for a quantitative study of cell adhesion, *J. Cell Sci.* **56**, 21–48.
32. Carpen, O., M.L. Dustin, T.A. Springer, J.A. Swafford, L.A. Beckett and J.P. Caulfield, 1991, Mobility and ultrastructure of large granular lymphocytes on lipid bilayers reconstituted with adhesion receptors LFA-1, ICAM-1 and two isoforms of LFA-3, *J. Cell Biol.* **115**, 861–871.
33. Carr, I., G. Everson, A. Rankin and J. Rutherford, 1970, The fine structure of the cell coat of the peritoneal macrophage and its role in the recongition of foreign material, *Z. Zellforsch. Microsk. Anat.* **105**, 339–349.
34. Chien, S., G.W. Schmid-Schönbein, K.L.P. Sung, E.A. Schmalzer and R. Skalak, 1984, Viscoelastic properties of leukocytes, in: *White Cell Mechanics – Basic Science and Clinical Aspects*, eds H.J. Meiselman, M.A. Lichtman and P.L. LaCelle (Alan Liss, New York) pp. 19–51.
35. Christink, E.R., M.A. Luscher, B.H. Barber and D.B. Williams, 1991, Peptide binding to class I MHC on living cells and quantitation of complexes required for CTL lysis, *Nature* **352**, 67–70.
36. Cook, G.M.W., 1976, Techniques for the analysis of membrane carbohydrates, in: *Biochemical Analysis of Membranes*, ed. A.H. Madden (Chapman and Hall, London) pp. 283–351.
37. Corri, W.D. and V. Defendi, 1981, Centrifugal assessment of cell adhesion, *J. Biochem. Biophys. Med.* **4**, 29–38.
38. Cozens-Roberts, C., D.A. Lauffenburger and J.A. Quinn, 1990, Receptor-mediated cell attachment and detachment kinetics. I – Probabilistic model and analysis, *Biophys. J.* **58**, 841–856.
39. Curtis, A.S.G., 1967, *The Cell Surface: Its Molecular Role in Morphogenesis* (Logo Press, Academic Press, New York).
40. Curtis, A.S.G., 1988, The data on cell adhesion, in: *Physical Basis of Cell-Cell Adhesion*, ed. P. Bongrand (CRC Press, Boca Raton, FL) pp. 207–225.
41. Curtis, A.S.G. and J.V. Forrester, 1984, The competitive effect of serum proteins on cell adhesion, *J. Cell Sci.* **71**, 17–35.
42. Curtis, A.S.G. and J.M. Lackie, 1991, *Measuring Cell Adhesion* (Wiley, New York).
43. Curtis, A.S.G., M. McGrath and L. Gasmí, 1992, Localised application of an activating signal to a cell: Experimental use of fibronectin bound to beads and the implications for mechanisms of adhesion, *J. Cell Sci.* **101**, 427–436.

44. David, G., V. Lories, A. Heremans, B. van der Schuerent, J.J. Cassiman and H. van den Bergh, 1989, Membrane-associated chondroitin sulfate proteoglycans of human lung fibroblast, *J. Cell Biol.* **108**, 1165–1175.
45. de Biasio, R.L., L.L. Wang, G.W. Fisher and D.L. Taylor, 1988, The dynamic distribution of fluorescent analogues of actin and myosin in protrusions at the leading edge of migrating swiss 3T3 fibroblasts, *J. Cell Biol.* **107**, 2631–2645.
46. de Gennes, P.G., 1979, *Scaling Concepts in Polymer Physics* (Cornell University Press, Ithaca).
47. de Gennes, P.G., 1987, Polymer at interfaces: A simplified view, *Adv. Colloid Interface Sci.* **27**, 189–209.
48. de Gennes, P.G., 1988, Model polymer at interfaces, in: *Physical Basis of Cell-Cell Adhesion*, ed. P. Bongrand (CRC Press, Boca Raton, FL) pp. 39–60.
49. Dembo, M., D.C. Torney, K. Saxman and D. Hammer, 1988, The reaction-limited kinetics of membrane-to-surface adhesion and detachment, *Proc. R. Soc. London Ser. B* **234**, 55–83.
50. de Petris, S., 1978, Preferential distribution of surface immunoglobulins on microvilli, *Nature* **272**, 66–68.
51. Derjaguin, B.V., V.M. Muller and Y.D. Toporov, 1975, Effect of contact deformations on the adhesion of particles, *J. Colloid Interface Sci.* **115**, 480–492.
52. Detmers, P.A., S.D. Wright, E. Olsen, B. Kimball and Z.A. Cohn, 1987, Aggregation of complement receptors of human neutrophils in the absence of ligand, *J. Cell Biol.* **105**, 1137–1145.
53. Doi, M. and S.F. Edwards, 1988, *The Theory of Polymer Dynamics* (Clarendon Press, Oxford).
54. Dolan, A.K. and S.F. Edwards, 1974, Theory of the stabilization of colloids by adsorbed polymer, *Proc. Roy. Soc.* **A337**, 509–516.
55. Dolan, A.K. and S.F. Edwards, 1975, The effect of excluded volume on polymer dispersant action, *Proc. Roy. Soc.* **A343**, 427–442.
56. Dong, C., R. Skalak, K.L.P. Sung, G.W. Schmid-Schönbein and S. Chien, 1988, Passive deformation analysis of human leucocytes, *J. Biomech. Eng.* **110**, 27–36.
57. Easty, G.C., D.M. Easty and E.J. Ambrose, 1960, Studies of cellular adhesiveness, *Exp. Cell Res.* **19**, 539–548.
58. Edidin, M., S.C. Kuo and M.P. Sheetz, 1992, Lateral movement of membrane glycoproteins restricted by dynamic cytoplasmic barriers, *Science* **254**, 1379–1382.
59. Edidin, M. and M. Zuniga, 1984, Lateral diffusion of wild-type and mutant Ld antigens in L cells, *J. Cell Biol.* **99**, 2333–2335.
60. Einstein, A., 1956, *Investigations of the Theory of Brownian Movement* (Dover, New York).
61. Elias, H., A. Hennig and E. Schwartz, 1971, Stereology: Application to biomedical research, *Physiol. Rev.* **51**, 158–200.
62. Engel, J., E. Odermatt and A. Engel, 1981, Shapes, domain organizations and flexibility of laminin and fibronectin, two multifunctional proteins of the extracellular matrix, *J. Mol. Biol.* **150**, 97–120.
63. Erickson, C.A. and J.P. Trinkaus, 1976, Microvilli and blebs as sources of reserve surface membrane during cell spreading, *Exp. Cell Res.* **99**, 375–384.
64. Evans, E.A., 1985, Detailed mechanics of membrane-membrane adhesion and separation. I – Continuum of molecular cross-bridges, *Biophys. J.* **48**, 175–183.
65. Evans E.A., 1985, Detailed mechanics of membrane-membrane adhesion and separation. II – Discrete kinetically trapped molecular cross-bridges, *Biophys. J.* **48**, 175–183.
66. Evans, E., D. Berk and A. Leung, 1991, Detachment of agglutinin-bonded red blood cells. I – Forces to rupture molecular point attachments, *Biophys. J.* **59**, 838–848.
67. Evans, E.A. and B. Kukan, 1984, Passive material behavior of granulocytes based on large deformation and recovery after deformation test, *Blood* **64**, 1028–1035.
68. Evans, E.A. and A. Leung, 1984, Adhesivity and rigidity of red blood cell membrane in relation to WGA binding, *J. Cell Biol.* **98**, 1201–1208.
69. Evans, E.A. and M. Metcalfe, 1984, Free energy potential for aggregation of mixed PC:PS lipid vesicles in glucose polymer (dextran), *Biophys. J.* **45**, 715–720.
70. Evans, E.A. and V.A. Parsegian, 1986, Thermal-mechanical fluctuations enhance repulsion between bimolecular layers, *Proc. Nat. Acad. Sci. USA* **83**, 7132–7136.

71. Evans, E.A. and R. Skalak, 1980, *Mechanics and Thermodynamics of Biomembranes* (CRC Press, Boca Raton, FL).
72. Evans, E.A. and A. Yeung, 1989, Apparent viscosity and cortical tension of blood granulocytes determined by micropipet aspiration, *Biophys. J.* **56**, 151–160.
73. Eyring, E., J. Walter and G.E. Kimball, 1944, *Quantum Chemistry* (Wiley, New York).
74. Flanagan, I. and G.L.E. Koch, 1978, Cross-linked surface Ig attaches to actin, *Nature* **273**, 278–281.
75. Flory, P.J. 1981, *Principles of Polymer Chemistry* (Cornell University Press, Ithaca).
76. Foa, C., J.L. Mège, C. Capo, A.M. Benoliel, J.R. Galindo and P. Bongrand, 1988, T-cell mediated cytotoxicity: Analysis of killer and target deformability and deformation during conjugate formation, *J. Cell Sci.* **89**, 561–573.
77. Foxall, C., S.R. Watson, D. Dowbenko, C. Fennie, L.A. Lasky, M. Kiso, A. Hasegawa, D. Asa and B.K. Brandley, 1992, The three members of the selectin receptor family recognize a common carbohydrate epitope, the sialyl lewis oligosaccharide, *J. Cell Biol.* **117**, 895–902.
78. Francis, G.W., L.R. Fisher, R.A. Gamble and D. Gingell, 1987, Direct measurement of cell detachment on single cells, using a new electromechanical method, *J. Cell Sci.* **87**, 519–523.
79. Frojmovic, M., K. Longmire and T.G. van de Ven, 1990, Long range interactions in mammalian platelet aggregation. II – The role of platelet pseudopod number and length, *Biophys. J.* **58**, 309–318.
80. Gennis, R.B., 1989, *Biomembranes – Molecular Structure and Function* (Springer, New York).
81. Gingell, D. and I. Todd, 1980, Red blood cell adhesion. II – Interferometric examination of the interaction with hydrocarbon oil and glass, *J. Cell Sci.* **41**, 135–149.
82. Goldman, A.J., R.G. Cox and H. Brenner, 1967, Slow viscous motion of a sphere parallel to a plane wall. II – Couette flow, *Chem. Eng. Sci.* **22**, 653–660.
83. Golstein, P. and E.E. Smith, 1976, The lethal hit stage of mouse T and non T cell mediated cytotoxicity: Differences in cation requirements and characterization of an analytical ‘cation pulse’ method.
84. Good, R.J., 1977, Surface free energy of solids and liquids: Thermodynamics, molecular forces and structure, *J. Colloid Interface Sci.* **59**, 398–419.
85. Greenwood, J.A. and J.B.P. Williamson, 1966, Contact of nominally flat surfaces, *Proc. R. Soc. London Ser. A* **295**, 300–319.
86. Grimm, E., Z. Price and B. Bonavida, 1979, Studies on the induction and expression of T cell-mediated immunity. III. Effector-target junctions and target cell membrane disruption during cytotoxicity, *Cell Immunol.* **46**, 77–99.
87. Grinnell, F. and M.K. Feld, 1982, Fibronectin adsorption on hydrophilic and hydrophobic surfaces detected by antibody binding and analyzed during cell adhesion in serum-containing medium, *J. Biol. Chem.* **257**, 4888–4893.
88. Hammer, D.A. and D.A. Lauffenburger, 1987, A dynamical model for receptor-mediated adhesion to surfaces, *Biophys. J.* **52**, 475–487.
89. Harris, A.K., P. Wild and D. Stopak, 1980, Silicone rubber substrata: A new wrinkle in the study of cell locomotion, *Science* **208**, 177–179.
90. Haynes, B.F., M.J. Telen, L.P. Hale and S.M. Denning, 1989, CD44 – A molecule involved in leukocyte adherence and T cell activation, *Immunol. Today* **10**, 423–428.
91. Hedman, K., S. Johansson, T. Vartio, L. Kjellén, A. Vaheri and H. Hook, 1982, Structure of the pericellular matrix: Association of heparan and chondroitin sulfates with fibronectin-procollagen fibres, *Cell* **28**, 603–671.
92. Hellfrich, W., 1978, Steric interaction of fluid membranes in multilayer systems, *Z. Naturforsch.* **33a**, 305–315.
93. Henkart, P.A., 1985, Mechanisms of lymphocyte-mediated cytotoxicity, *Annu. Rev. Immunol.* **3**, 31–58.
94. Hiramoto, Y., 1969, Mechanical properties of the protoplasm of the sea urchin egg. I – Unfertilized egg, *Exp. Cell Res.* **56**, 201–208.
95. Horn, R.G., J.N. Israelachvili and F. Pribac, 1987, Measurement of the deformation and adhesion of solids in contact, *J. Colloid Interface Sci.* **115**, 480–492.

96. Horoyan, M., A.M. Benoliel, C. Capo and P. Bongrand, 1990, Localization of calcium and micro-filament changes in mechanically stressed cells, *Cell Biophys.* **17**, 243–256.
97. Hynes, R.O., 1992, Integrins: Versatility, *n* modulation and signaling in cell adhesion, *Cell* **69**, 11–25.
98. Israelachvili, J., 1991, *Intermolecular and Surface Forces* (Academic Press, New York).
99. Israelachvili, J. and R. Pashley, 1982, The hydrophobic interaction is long-range decaying exponentially with distance, *Nature* **300**, 341–342.
100. Israelachvili, J., R.K. Tandon and L.R. White, 1979, Measurement of forces between two mica surfaces in aqueous poly (ethyleneoxide) solutions, *Nature* **277**, 120–121.
101. Johnson, K.L., K. Kendall and A.D. Roberts, 1971, Surface energy and the contact of elastic solids, *Proc. R. Soc. London A* **324**, 301–313.
102. Kabat, E.A., 1968, *Structural Concepts in Immunology and Immunochemistry* (Holt, Rinehart and Winston, New York).
103. Kalina, M. and G. Berke, 1976, Contact regions of cytotoxic T lymphocyte-target cell conjugates, *Cell Immunol.* **25**, 41–51.
104. Kinloch, A.J., 1980, The science of adhesion – Part I: Surface and interfacial aspects, *J. Mater. Sci.* **15**, 2141–2166.
105. Knutton, S.K., M.C.B. Sumner and C.A. Pasternak, 1975, Role of microvilli in surface charge of synchronized P815Y mastocytoma cells, *J. Cell Biol.* **66**, 568–576.
106. Kolodney, M.S. and R.B. Wysolmerski, 1992, Isometric contraction by fibroblasts and endothelial cells in tissue culture: A quantitative study, *J. Cell Biol.* **177**, 73–82.
107. Koppel, D.E., M.P. Sheetz and M. Schindler, 1981, Matrix control of protein diffusion in biological membranes, *Proc. Nat. Acad. Sci. USA* **78**, 3576–3580.
108. Kraemer, P.H., 1979, Mucopolysaccharides: Cell biology and malignancy, in: *Surfaces of Normal and Malignant Cells*, ed. R.O. Hynes (Wiley, New York).
109. Kupfer, A. and S.J. Singer, 1989, Cell biology of cytotoxic and helper T cell functions, *Annu. Rev. Immunol.* **7**, 309–338.
110. Langlet, C., G.A. Neil and L.A. Sherman, 1987, The mechanism of anti-Lyt2 inhibition of antibody-directed lysis by cytotoxic T lymphocytes, *J. Immunol.* **139**, 3590–3596.
111. Lawrence, M.B. and T.A. Springer, 1991, Leukocytes roll on a selectin at physiologic flow rates: Distinction from and prerequisite for adhesion through integrins, *Cell* **65**, 859–873.
112. LeBouteiller, P.P., Z. Mishal, F.A. Lemonnier and F.M. Kourilsky, 1983, Quantification by flow cytometry of HLA class I molecules at the surface of murine cells transformed by cloned HLA gene, *J. Immunol. Methods* **61**, 301–315.
113. Lehninger, A., 1973, *Biochimie* (Flammarion, Paris).
114. Levine, Y.K., 1972, Physical studies of membrane structure, *Prog. Biophys. Mol. Biol.* **24**, 1–74.
115. Lipscomb, M.F., K.V. Holmes, E.S. Vitetta, U. Hammerling and J.W. Uhr, 1975, Cell surface immunoglobulin. XII – Localization of immunoglobulin on muring lymphocytes by scanning immunoelectron microscopy, *Eur. J. Immunol.* **5**, 255–259.
116. Lis, L.J., M. Mcalister, N. Fuller, R.D. Rand and V.A. Parsegian, 1982, Interaction between neutral phospholipid bilayer membranes, *Biophys. J.* **37**, 657–666.
117. Livnek, E., M. Benveniste, R. Prywes, S. Felder, Z. Kam and J. Schlessinger, 1986, Large deletions in the cytoplasmic kinase domain of the epidermal growth factor receptor do not affect its lateral mobility, *J. Cell Biol.* **103**, 327–331.
118. Luckham, P.F. and J. Klein, 1984, Forces between mica surfaces bearing adsorbed polyelectrolytes, *J. Chem. Soc. Faraday Trans.* **80**, 865–878.
119. Makita, A. and H. Shimojo, 1973, Polysaccharides of SV40-transformed green monkey kidney cells, *Biochim. Biophys. Acta* **304**, 571–574.
120. Margolis, L.B., E.V. Dyatovitskaya and L.D. Bergelson, 1978, Cell-lipid interaction: Cell attachment to lipid substrates, *Exp. Cell Res.* **111**, 454–457.
121. Margolis, L.B., A.N. Tikhonov and E.Y. Vasilieva, 1980, Platelet adhesion to fluid and solid phospholipid membranes, *Cell* **19**, 189–195.
122. Martinez-Palomo, A., 1970, The surface coats of animal cells, *Int. Rev. Cytol.* **29**, 29–75.

123. Mayrovitz, H.N., 1992, Leukocyte rolling. A prominent feature of venules in intact skin of anesthetized hairless mice, *Am. J. Physiol.* **262**, H157–H161.
124. McClay, D.R., G.M. Wessel and R. B. Marchase, 1981, Intercellular recognition: Quantitation of initial binding events, *Proc. Nat. Acad. Sci. USA* **78**, 4975–4979.
125. McKeever, P.E. 1974, Methods to study pulmonary alveolar macrophage adherence: Micromanipulation and quantitation, *J. Reticuloendothelial Soc.* **16**, 313–317.
126. McKeown-Longo, P.J. and D.F. Mosher, 1983, Binding of plasma fibronectin to cell layers of human skin fibroblasts, *J. Cell Biol.* **97**, 466–472.
127. Mège, J.L., C. Capo, P. André, A.M. Benoliel and P. Bongrand, 1990, Mechanisms of leukocyte adhesion, *Biorheology* **27**, 433–444.
128. Mège, J.L., C. Capo, A.M. Benoliel and P. Bongrand, 1986, Determination of binding strength and kinetics of binding initiation – a model study made on the adhesive properties of P388D1 macrophage-like cells, *Cell Biophys.* **8**, 141–160.
129. Mège, J.L., C. Capo, A.M. Benoliel and P. Bongrand, 1987, Use of contour analysis to evaluate the affinity between macrophages and glutaraldehyde-treated erythrocytes, *Biophys. J.* **52**, 177–186.
130. Mège, J.L., C. Capo, A.M. Benoliel, C. Foa and P. Bongrand, 1984, Nonspecific cell surface properties: Contact angle of water on dried cell monolayers, *Immunol. Commun.* **13**, 211–227.
131. Mège, J.L., C. Capo, A.M. Benoliel, C. Foa and P. Bongrand, 1985, Study of cell deformability by a simple method, *J. Immunol. Methods* **82**, 3–15.
132. Mège, J.L., C. Capo, A.M. Benoliel, C. Foa, J.R. Galindo and P. Bongrand, 1986, Quantification of cell surface roughness: A method for studying cell mechanical and adhesive properties, *J. Theoret. Biol.* **119**, 147–160.
133. Mehrishi, J.N., 1972, Molecular aspects of the mammalian cell surface, *Prog. Biophys. Mol. Biol.* **25**, 3–70.
134. Meiselman, H.J., M.A. Lichtman and P.L. LaCelle, 1984, *White Cell Mechanics: Basic Sciences and Clinical Aspects* (Alan Liss, New York).
135. Michl, J., M.M. Pieczonka, J.C. Unkeless, G.I. Bell and S.C. Silverstein, 1983, Fc Receptor modulation in mononuclear phagocytes maintained on immobilized immune complexes occurs by diffusion of the receptor molecule, *J. Exp. Med.* **157**, 2121–2139.
136. Mosher, D.F., F.J. Fogerty, M.A. Chernousov and E.L.R. Barry, 1991, Assembly of fibronectin into extracellular matrix, *Ann. NY Acad. Sci.* **614**, 167–180.
137. Napper, D.H., 1983, *Polymeric Stabilization of Colloid Dispersions* (Academic Press, London).
138. Neumann, A.W., D.R. Absolom, C.J. van Oss and W. Zingg, 1979, Surface thermodynamics of leukocyte and platelet adhesion to polymer surfaces, *Cell Biophys.* **1**, 79–92.
139. Norment, A.M., R.D. Salter, P. Parham, V.H. Engelhard and D.R. Littman, 1988, Cell-cell adhesion mediated by CD8 and MHC class I molecules, *Nature* **336**, 79–81.
140. Pardi, R., L. Inverardi and J.R. Bender, 1992, Regulatory mechanisms in leukocyte adhesion: Flexible receptors for sophisticated travelers, *Immunol. Today* **13**, 224–230.
141. Pasternak, C. and E.L. Elson, 1985, Lymphocyte mechanical response triggered by cross-linking surface receptors, *J. Cell Biol.* **100**, 860–872.
142. N.O. Petersen, W.B. McConnaugley and E.L. Elson, 1982, Dependence of locally measured cellular deformability on position of the cell, temperature and cytochalasin B, *Proc. Nat. Acad. Sci. USA* **79**, 5327–5331.
143. Picker, L.J., R.A. Warnock, C.K. Arburns, C.M. Doershnik, E.L. Berg and E.C. Butcher, 1991, The neutrophil selectin LECAM-1 presents carbohydrate ligands to the vascular selectin, *Cell* **66**, 921–933.
144. Piersbacher, M.D. and E. Ruoshlahti, 1984, Cell attachment activity of fibronectin can be duplicated by small synthetic fragments of the molecule, *Nature* **309**, 30–33.
145. Podack, E.R. and M.G. Lichtenheld, 1991, A central role of perforin in cytolysis?, *Annu. Rev. Immunol.* **9**, 129–157.
146. Rees, D.A., C.W. Lloyd and D. Thom, 1977, Control of grip and stick in cell adhesion through lateral relationships of membrane glycoproteins, *Nature* **267**, 124–128.

147. Robbin, R., S.O. Albert, N.A. Gelb and P.H. Black, 1975, Cell surface changes correlated with density dependent growth inhibition. Glycosaminoglycan metabolism in 3T3, SV3T3 and conA-selected revertant cells, *Biochemistry* **14**, 347–357.
148. Rothstein, T.L., M. Mage, G. Jones and L.L. McHugh, 1978, Cytotoxic T lymphocyte sequential killing of immobilized allogeneic tumor target cells measured by time lapse microcinematography, *J. Immunol.* **121**, 1652–1656.
149. Rutishauser, U., A. Acheson, A.K. Hall, D.M. Mann and J. Sunshine, 1988, The neural cell adhesion molecule (NCAM) as a regulator of cell-cell interactions, *Science* **240**, 53–57.
150. Ryan, T.A., J. Myers, D. Holowka, B. Baird and W.W. Webb, 1988, Molecular constraint on the cell surface, *Science* **239**, 61–64.
151. Schackenraad, J.M., H.J. Busscher, C.R.H. Wildevuur and J. Arends, 1988, Thermodynamic aspects of cell spreading on solid substrata, *Cell Biophys.* **13**, 75–91.
152. Schlessinger, J., L.S. Barak, G.G. Hammer, K.M. Yamada, I. Pastan, W.W. Webb and E.L. Elson, 1977, Mobility and distribution of a cell surface glycoprotein and its interaction with other membrane components, *Proc. Nat. Acad. Sci. USA* **74**, 2909–2913.
153. Schmid-Schönbein, G.W., K.L.P. Sung, H. Tozeren, R. Skalak and S. Chien, 1981, Passive mechanical properties of human leucocytes, *Biophys. J.* **36**, 243–256.
154. Schmid-Schönbein, G.W., S. Usami, R. Skalak and S. Chien, 1980, The interaction of leukocytes and erythrocytes in capillary and post-capillary vessels, *Microvas. Res.* **19**, 45–70.
155. Schubert, D. and M. Lacorbière, 1980, A role of secreted glycosaminoglycans in cell-substratum adhesion, *J. Biol. Chem.* **255**, 11564–11569.
156. Schürch, S., D.F. Gerson and D.J.L. McIver, 1981, Determination of cell-medium interfacial tensions from contact angles in aqueous polymer systems, *Biochim. Biophys. Acta* **640**, 557–571.
157. Scullion, B.F., Y. Hou, L. Puddington, J.K. Rose and K. Jacobson, 1987, Effect of mutations in three domains of the vesicular stomatitis viral glycoprotein on its lateral diffusion in the plasma membrane, *J. Cell Biol.* **105**, 69–75.
158. Shaw, S., G.E. Gunther-Luce, R. Quinones, R.E. Gress, T.A. Springer and M.E. Sanders, 1986, Two antigen-independent adhesion pathways used by human cytotoxic T cell clones, *Nature* **323**, 262–264.
159. Soderquist, M.E. and A.G. Walton, 1980, Structural changes in proteins adsorbed on polymer surfaces, *J. Colloid Interface Sci.* **75**, 386–397.
160. Springer, T.A., 1990, Adhesion receptors of the immune system, *Nature* **346**, 425–434.
161. Staunton, D.E., M.L. Dustin, H.P. Erickson and T.A. Springer, 1990, The arrangement of the immunoglobulin-like domains of ICAM-1 and the binding sites for LFA-1 and rhinovirus, *Cell* **61**, 243–254.
162. Stolberg, J. and S.E. Fraser, 1988, Acetylcholine receptors and concanavalin A binding sites on culture *Xenopus* muscle cells. Electrophoresis, diffusion and aggregation, *J. Cell Biol.* **107**, 1397–1408.
163. Sugimoto, Y., 1981, Effect on the adhesion and locomotion of mouse fibroblasts by their interaction with differently charged substrates. A quantitative study by ultrastructural methods, *Exp. Cell Res.* **135**, 39–45.
164. Sung, K.L.P., C. Dong, G.W. Schmid-Schönbein, S. Chien and R. Skalak, 1988, Leukocyte relaxation properties, *Biophys. J.* **54**, 331–336.
165. Sung, K.L.P., L.A. Sung, M. Crimmins, S.J. Burakoff and S. Chien, 1986, Determination of junction avidity of cytolytic T cell and target cell, *Science* **234**, 1405–1408.
166. Tangelder, G.J. and K.E. Arfors, 1991, Inhibition of leukocyte rolling in venules by protamine and sulfated polysaccharides, *Blood* **77**, 1565–1571.
167. Taniguchi, N., I. Nanba and S. Kozuyumi, 1974, Characterization of glycosaminoglycans in human leucocytes, *Biochem. Med.* **11**, 217–226.
168. Tank, D.W., E.S. Wu and W.W. Webb, 1982, Enhanced molecular diffusibility in muscle membrane blebs: release of lateral constraints, *J. Cell Biol.* **92**, 207–212.
169. Tha, S.P., J. Shuster and H.L. Goldsmith, 1986, Interaction forces between red cells agglutinated by antibody. II – Measurement of hydrodynamic force of breakup, *Biophys. J.* **50**, 1117–1126.

170. Tissot, O., A. Pierres, C. Foa, M. Delaage and P. Bongrand, 1992, Motion of cells sedimenting on a solid surface in a laminar shear flow, *Biophys. J.* **61**, 204–215.
171. Tozeren, A., 1990, Cell-cell conjugation – transient analysis and experimental implication, *Biophys. J.* **58**, 641–652.
172. Tozeren, A., K.L.P. Sung and S. Chien, 1989, Theoretical and experimental studies on cross bridge migration during cell disaggregation, *Biophys. J.* **55**, 479–487.
173. Tran-Son-Tay, R., D. Needham, A. Yeung and R.M. Hochmuth, 1991, Time-dependent recovery of passive neutrophils after large deformation, *Biophys. J.* **60**, 856–866.
174. Unanue, E.R., W.D. Perkins and M.J. Karnovsky, 1972, Ligand-induced movement of lymphocyte membrane macromolecules. I – Analysis by immunofluorescence and ultrastructural radioautography, *J. Exp. Med.* **136**, 885–906.
175. Valentine, R.C. and N.M. Green, 1967, Electron microscopy of an antibody-hapten complex, *J. Mol. Biol.* **27**, 615–617.
176. Van Oss, C.J., 1991, Interaction forces between biological and other polar entities in water: How many different primary forces are there?, *J. Disp. Sci. Technol.* **12**, 201–220.
177. Van Oss, C.J., M.K. Chaudury and R.J. Good, 1987, Monopolar surfaces, *Adv. Colloid Surface Sci.* **28**, 35–64.
178. Vogel, K.G. and R.O. Kelley, 1977, Cell surface glycosaminoglycans: Identification and organization in cultured human embryo fibroblasts, *J. Cell Physiol.* **92**, 469–480.
179. Vogler, E.A., 1988, Thermodynamics of short term cell adhesion in vitro, *Biophys. J.* **53**, 759–769.
180. Wade, W.F., J.H. Freed and M. Edidin, 1989, Translational diffusion of class II major histocompatibility complex molecules is constrained by their cytoplasmic domains, *J. Cell Biol.* **109**, 3325–3331.
181. Wagner, H. and M. Rollinghoff, 1974, T cell-mediated cytotoxicity: discrimination between antigen recognition, lethal hit and cytolysis phase, *Eur. J. Immunol.* **4**, 745–750.
182. Wegener, A.M.K., F. Letourneur, A. Hoeveler, T. Brocker, F. Luton and B. Malissen, 1992, The T cell receptor/CD3 complex is composed of at least two autonomous transduction molecules, *Cell* **68**, 83–95.
183. Weiller, N.K., 1974, Visualization of concanavalin A binding sites with scanning electron microscopy, *J. Cell Biol.* **63**, 699–707.
184. Weiss, P. and B. Garber, 1952, Shape and movements of mesenchyme cells as function of the physical structure of the medium. Contribution to a quantitative morphology, *Proc. Nat. Acad. Sci. USA* **38**, 264–280.
185. Wier, M. and M. Edidin, 1988, Constraint of the translational diffusion of a membrane glycoprotein by its external domain, *Science* **242**, 412–414.
186. Willingham, M.C. and I. Pastan, 1975, Cyclic AMP modulates microvillus formation and agglutinability in transformed and normal mouse fibroblasts, *Proc. Nat. Acad. Sci. USA* **72**, 1203–1267.
187. Winzler, R.J., 1970, Carbohydrates in cell surface, *Int. Rev. Cytol.* **29**, 77–125.
188. Woods, A., M. Hook, L. Kjellen, C.G. Smith and D.A. Rees, 1984, Relationship of heparan sulfate proteoglycans to the cytoskeleton and extracellular matrix of cultured fibroblasts, *J. Cell Biol.* **99**, 1743–1753.
189. Yanagishita, M. and V.C. Hascall, 1992, Cell surface heparan sulfate proteoglycans, *J. Biol. Chem.* **267**, 9451–9454.
190. Zhang, F., B. Crise, B. Su, Y. Hou, J.K. Rose, A. Bothwell and K. Jacobson, 1991, Lateral diffusion of membrane-spanning and glycosylphosphatidyl inositol-linked proteins: Towards establishing rules governing the lateral mobility of membrane molecules, *J. Cell Biol.* **119**, 75–84.
191. Zimmerman, G.A., S.M. Prescott and T.M. McIntyre, 1992, Endothelial cell interactions with granulocytes: Tethering and signaling molecules, *Immunol. Today* **13**, 93–100.
192. Zurkhov, S.N., 1965, Kinetic concept of the strength of solids, *Int. J. Fract. Mech.* **1**, 311–323.
193. Kaplanski, G., C. Farnarier, O. Tissot, A. Pierres, A.M. Benociel, M.C. Alessi, S. Kaplanski and P. Bongrand, 1992, *Biophys. J.* **64**,